system, for example, locating the target gene under the *GAL* promoter and changing the carbon source of culture medium from galactose to glucose to suppress transcription. However, in this system, the target protein is depleted according to its natural half-life. Therefore, stable proteins such as ORC are depleted slowly, and thus other approaches seem necessary (*15*).

Creating a heat-inducible degron mutant is a very useful way to achieve rapid conditional degradation of a target protein. The N-terminal of the target protein is fused with the N-terminal fragment of mutated (temperature-sensitive) mouse dihydrofolate reductase (DHFR) gene, the so-called 'heat-inducible degron'. When cells are incubated at the non-permissive temperature (37°C), the fused protein is easily ubiquitinated, resulting in its rapid degradation by ubiquitin-proteasome system (*20*). Diffley and co-workers (*21–23*) improved this method by *GAL* promoter-regulated simultaneous overproduction of Ubr1p, the E3 ubiquitin ligase, which stimulates this degradation. This improvement has proved useful for genetic analysis of DNA replication-related proteins, such as Cdc45p, and the mini-chromosome maintenance complex of proteins (MCM). Kanemaki *et al.* (*24*) clearly showed that Mcm4p can be rapidly depleted in a heat-inducible degron mutant with the overproduction of Ubr1p, but not in cells with a genetic shut-off system. In this study, we constructed a heat-inducible degron mutant for each ORC subunit. Under non-permissive conditions (incubation at 37°C in the presence of galactose), each targeted subunit, and also other subunits of ORC, were rapidly degraded. All *orc* degron mutants showed a temperature-dependent galactose-stimulated growth defect. Block and release experiments using the *orc5* mutant showed that Orc5p (ORC) is necessary at late G1, rather than early G1 and G2/M phases, for the G1/S transition and pre-replicative complex (pre-RC) formation, suggesting that ORC functions as the initiator of chromosomal DNA in budding yeast.

MATERIALS AND METHODS

Strains, Plasmids and Medium—S. cerevisiae strains are listed in Table 1 (*25*). Cells were cultured in YP medium (1% yeast extract and 2% Bacto-peptone) containing 2% galactose, raffinose or glucose. Plasmids, pPW66R and pKL54, were gifts from Dr. Diffley. Plasmids, pRS404, pFA6a-3HA-*TRP1* and pFA6a-13Myc-*TRP1*, were from our laboratory stock.

The degron mutant for each *ORC* gene was constructed as described previously (*21, 23*). The plasmid pKL54 (*GAL-UBR1*) was digested with *Pme*I and transformed into W303-1A. The construct of the resultant strain (YYM101) was confirmed by colony PCR. DNA encoding the N-terminal region of each ORC subunit was then amplified by PCR and the amplified DNA was ligated into the *Hin*dIII-*Xho*I region of pPW66R. The resultant plasmid was digested with a single-cutting restriction enzyme and transformed into YYM101. The construction of resultant strains (YYM102–107) was confirmed by colony PCR.

Modification of the *ORC2* gene with 13Myc, or of the *ORC6* gene with 3HA (haemagglutinin, HA) was performed as described previously (*26*). PCR was performed using pFA6a-3HA-*TRP1* or pFA6a-13Myc-*TRP1* plasmid as template, with primers to the C-terminal region of the *ORC6* or *ORC2* genes, respectively. The amplified DNA was transformed into W303-1A, YYM104 or YYM106. The construction of resultant strains (YYM108–113) was confirmed by colony PCR.

Table 1. **Yeast strains**

Strain	Genotype	Reference
W303-1A	*Mata ade2-1 can1-100 his3-11,15 leu2-3,112 trp1-1 ura3-1*	Thomas and Rothstein (*25*)
YYM101	W303-1A *ubr1*Δ*::GAL-Myc-UBR1::HIS3*	This study
YYM102	YYM101 *orc1-td*	This study
YYM103	YYM101 *orc2-td*	This study
YYM104	YYM101 *orc3-td*	This study
YYM105	YYM101 *orc4-td*	This study
YYM106	YYM101 *orc5-td*	This study
YYM107	YYM101 *orc6-td*	This study
YYM108	W303-1A *ORC2-13Myc::TRP1*	This study
YYM109	W303-1A *ORC6-3HA::TRP1*	This study
YYM110	YYM104 *ORC2-13Myc::TRP1*	This study
YYM111	YYM104 *ORC6-3HA::TRP1*	This study
YYM112	YYM106 *ORC2-13Myc::TRP1*	This study
YYM113	YYM106 *ORC6-3HA::TRP1*	This study
YYM114	W303-1A *bar1*Δ*::TRP1*	This study
YYM115	YYM106 *bar1*Δ*::TRP1*	This study

Disruption of the *BAR1* gene in W303-1A and YY106 was performed as described previously (*27*). PCR of the *BAR1* gene was performed using pRS404 (a plasmid with *TRP1*) as template, and primers to the 5′ upstream region of the N-terminal or 3′ downstream region of the C-terminal. The amplified DNA was transformed into W303-1A or YYM106. The construct of resultant strains (YYM114–115) was confirmed by colony PCR.

Fluorescence-Activated Cell Sorter (FACS) Analysis—Samples were prepared as previously described (*15*) with some modifications. Cells were pelleted by centrifugation, washed with sterilized water and fixed in 70% ethanol for 12 h. Cells were again pelleted, re-suspended in 50 mM sodium citrate, sonicated for 1 min, treated with 0.25 mg/ml RNase A (SIGMA) for 1 h at 50°C and then with 1 mg/ml Proteinase K (Wako) for 1 h at 50°C. DNA was stained with 50 μg/ml of propidium iodide (SIGMA) and 20,000 cells from each sample were scanned with a FACSCalibur (Becton Dickinson).

Chromatin-Binding Analysis—Yeast spheroplasts were lysed with Triton X-100 and samples were processed into soluble (supernatant) and chromatin (insoluble precipitate) fractions by centrifugation (*15*). Equivalent amounts (total protein) of chromatin fractions were electrophoresed on 7.5% polyacrylamide gels containing SDS, transferred to PVDF membrane–and probed with monoclonal antibodies against Orc3p (SB3), Orc5p (SB5), Mcm2 (Mcm2–28), HA (12CA5) or Myc (9E10) (*28–31*).

Block and Release Experiments for Cell Cycle Progression—Yeast cells were cultured at 24°C to early log phase and cell cycle progression was blocked at the G1, S or G2/M phase by incubation with 0.05–5 μg/ml with α mating factor (α-factor) (SIGMA), 0.1 M

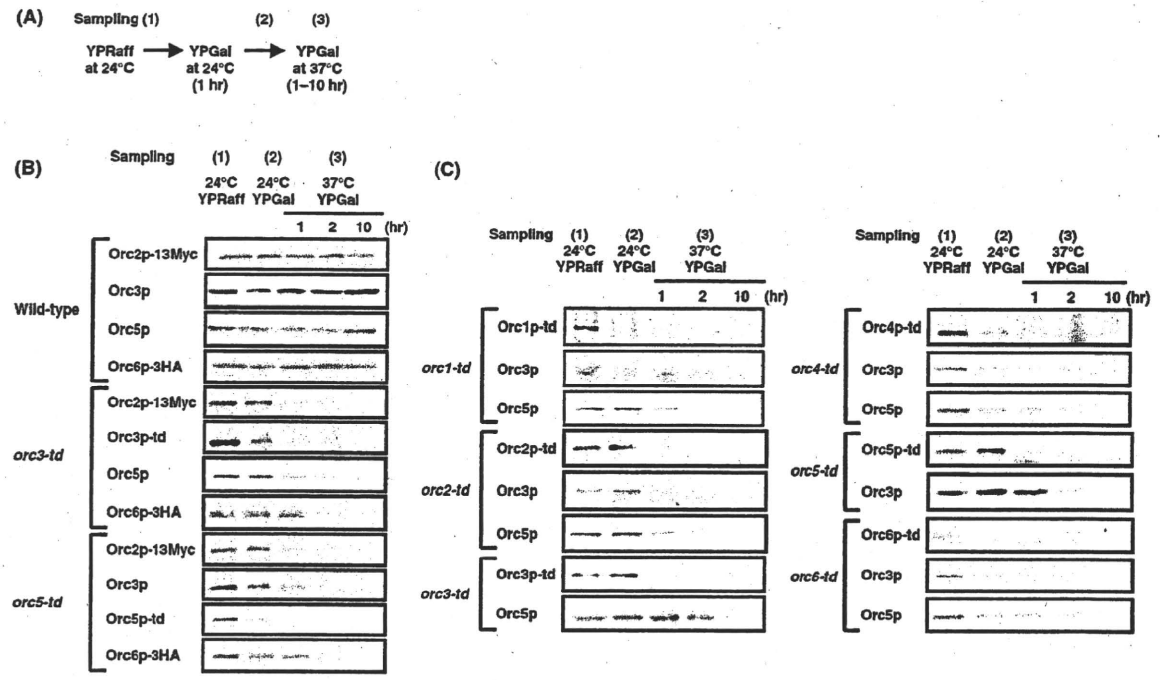

Fig. 1. **Degradation of ORC subunits in *orc* degron mutants.** (A) Experimental outline and timing of sampling. (B) W303-1A, YYM108, YYM109 (wild-type); YYM104, YYM110, YYM111 (*orc3-td*); and YYM106, YYM112, YYM113 (*orc5-td*) cells were cultured in YP medium with 2% raffinose (YPRaff) to logarithmic phase at 24°C, and then cultured in YP medium with 2% galactose (YPGal) for 1 h at 24°C. Cells were further incubated at 37°C in the same medium, and a small portion of culture was taken when indicated. Chromatin fractions were prepared and analysed by immunoblotting using monoclonal antibodies specific for Orc3p, Orc5p, Myc (for Orc2p-13Myc) and HA (for Orc6p-3HA and each td-subunit). (C) YYM102-107 (*orc1-td*, *orc2-td*, *orc3-td*, *orc4-td* *orc5-td* and *orc6-td*) cells were cultured and analysed as above.

hydroxyurea (HU) (SIGMA) or 3 μg/ml nocodazole (SIGMA), respectively. Cells were released from the block by washing and re-suspending in fresh medium without the blocking agents.

RESULTS

Construction of a Heat-inducible Degron Mutant for Each ORC Subunit—To achieve temperature- and galactose-dependent rapid degradation of the targeted subunit of ORC, we inserted the 'heat-inducible degron' sequence at the N-terminal of each subunit of ORC, and transformed a plasmid containing the *UBR1* gene under the *GAL* promoter. Pre-incubation of *orc* degron mutants at 24°C for 1 h in YP medium with galactose (Fig. 1A) stimulated the subsequent degradation of the targeted subunit at 37°C (data not shown), so we routinely performed this pre-incubation. As shown in Fig. 1B, in the *orc3* degron mutant (*orc3-td*), Orc3p disappeared within 1 h of temperature shift (from 24°C to 37°C). Furthermore, following Orc3p-degradation, other subunits (myc-tagged Orc2p, Orc5p, HA-tagged Orc6p) also disappeared (Fig. 1B). Degradation of Orc1p and Orc4p could not be tested, as antibodies against Orc1p and Orc4p did not work under our experimental conditions, and we could not insert any tag into either the *ORC1* gene or the *ORC4* gene. Similar results were obtained with the *orc5* degron mutant (*orc5-td*); rapid degradation of Orc5p and subsequent degradation of other subunits (myc-tagged Orc2p, Orc3p, HA-tagged Orc6p; Fig. 1B). We confirmed that in wild-type cells the amount of each subunit of ORC is constant under the experimental conditions used (Fig. 1B).

For other heat-inducible *orc* degron mutants (*orc1-td*, *orc2-td*, *orc4-td* and *orc6-td*), there was rapid degradation of each targeted subunit and subsequent degradation of other subunits (Orc3p and Orc5p; Fig. 1C). Based on these results, we concluded that we had constructed heat-inducible degron mutant for every ORC subunit. From the results in Fig. 1, it can be suggested that ORC becomes unstable when any one of its subunits is degraded.

Growth Phenotypes of the Heat-Inducible orc Mutants—The effect of incubation temperatures and galactose on growth of each *orc* degron mutant strain was tested on YP agar plates (Fig. 2A). Compared to wild-type cells, the growth of all mutants was slow at 37°C, especially with galactose. At 24°C, growth of mutants was indistinguishable from that of wild-type cells (Fig. 2A). Since the transformation of *UBR1*-expression plasmid (*GAL-UBR1*) into the wild-type strain did not affect growth (Fig. 2A), the inhibition seen in mutants must be due to degron-dependent degradation of the targeted subunit and other subunits.

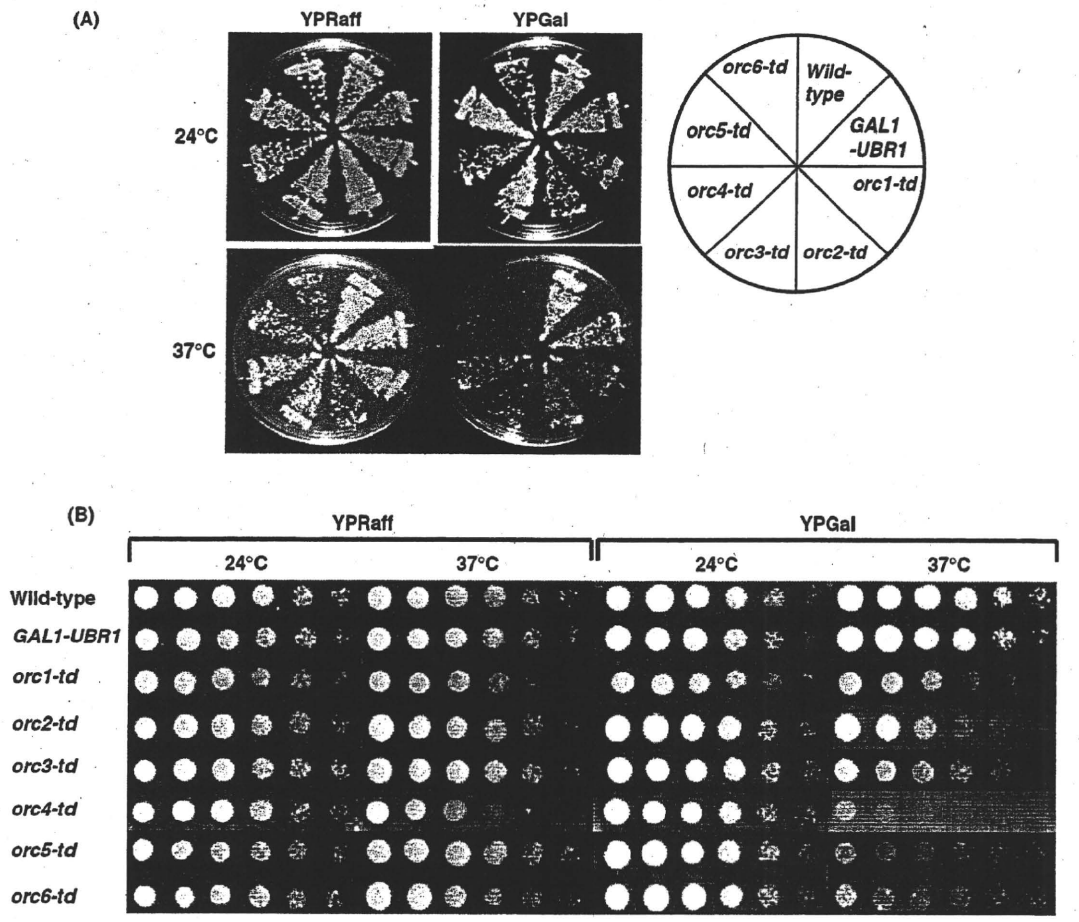

Fig. 2. **Growth phenotypes of ORC degron mutants.** W303-1A (wild-type), YYM101 (*GAL-UBR1*) and YYM102-107 (*orc1-td, orc2-td, orc3-td, orc4-td orc5-td* and *orc6-td*) cells were streaked on YP agar plates with 2% raffinose (YPRaff) or galactose (YPGal) and incubated at 24°C or 37°C for 2 days (A). Cell suspensions of each strain ($O.D._{600}$ = 1, 0.25, 0.13, 0.068, 0.034, 0.017; from left to right) were dropped onto YPRaff or YPGal and incubated at 24°C or 37°C for 2 days (B).

For quantitative monitoring of the growth of *orc* degron mutants, we performed a dilution assay. Every mutant showed a temperature-dependent and galactose-stimulated growth defect (Fig. 2B), which is consistent with the results in Fig. 2A. The extents of growth defects differed among the various *orc* degron mutants; *orc4, orc5* and *orc6* mutants showed relatively clear phenotype. We used some not all *orc* degron mutants in the following experiments.

Cell Cycle Progression in the Heat-Inducible orc Mutants—The results in Fig. 2 indicate that under the non-permissive conditions the mutants have defects in cell cycle progression. To determine which phase of the cell cycle is blocked, *orc3* and *orc5* mutants and wild-type cells were asynchronously grown at 24°C in YP medium with raffinose, then with galactose, the incubation temperature was shifted to 37°C, and their DNA contents were determined by FACS analysis (Fig. 3A). Compared to the wild-type cells, the proportion of cells with nearly 2C DNA content increased over time in *orc3* and *orc5* mutants (Fig. 3B), suggesting that most cells were blocked in late S phase or G2/M phase. This accumulation was observed earlier in the *orc5* mutant than in the *orc3* mutant, which is consistent with the greater growth defect in *orc5* mutant (Fig. 2B). The transformation of *UBR1*-expression plasmid into wild-type cells did not affect the cell cycle progression (Fig. 3B), suggesting that it is the degron-dependent degradation of ORC, which is responsible for this defect of cell cycle progression.

Eukaryotic cells have checkpoint systems, which detect DNA damage and defects in DNA replication and stop cell cycle progression (*32, 33*). Phosphorylation of Rad53p plays an important role in the checkpoint systems, and in some temperature-sensitive *orc* mutants Rad53p was phosphorylated at non-permissive temperatures (*32–34*). Thus, checkpoint systems may become induced in *orc* degron mutants under non-permissive conditions. We monitored Rad53p phosphorylation in the *orc5* mutant by immunoblotting under the same conditions as the FACS analysis. As shown in Fig. 3C, after incubation in

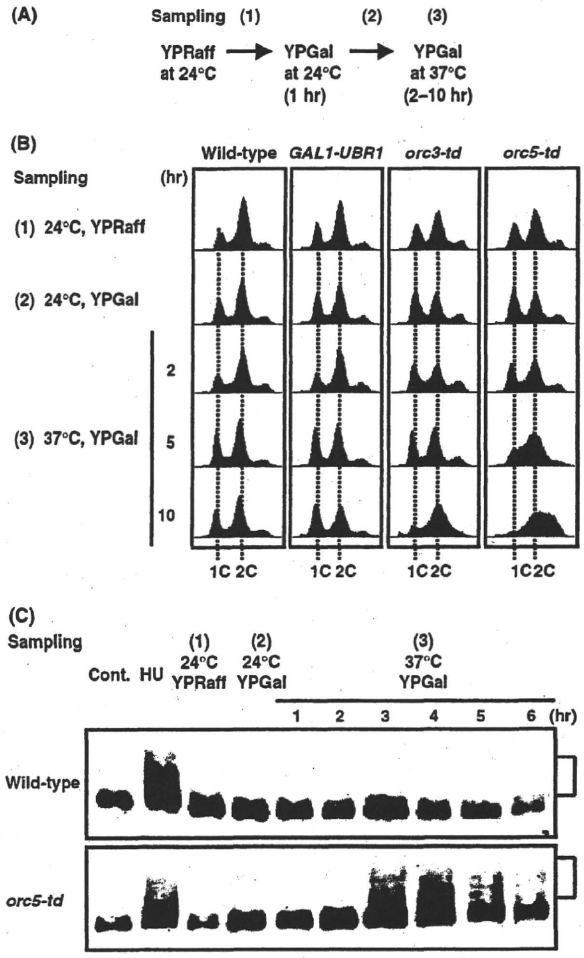

Fig. 3. **Cell cycle progression and phosphorylation of Rad53p in the *orc5* degron mutant.** W303-1A (wild-type), YYM101 (*GAL-UBR1*), YYM104 (*orc3-td*) and YYM106 (*orc5-td*) cells were cultured in YP medium with 2% raffinose (YPRaff) to logarithmic phase at 24°C and then cultured in YP medium with 2% galactose (YPGal) for 1 h at 24°C and finally in the same medium at 37°C. A small portion of culture was taken when indicated. (A) Experimental outline and timing of sampling. (B) Cellular DNA contents analysed by FACS. (C) Whole-cell extracts were analysed by immunoblotting with monoclonal antibody for Rad53p. For control experiments, wild-type cells were cultured for 2 h at 24°C in YPRaff with hydroxyurea (HU) or without it (Cont.). Phosphorylated forms of Rad53p are shown by an asterisk.

non-permissive conditions, the upper-shifted band of Rad53p increased in the *orc5* mutant, but not in wild-type cells. Similar increases were observed in wild-type cells treated with HU. These results suggest that checkpoint systems are induced when Orc5p (ORC) is degraded, and the defect of cell cycle progression in the *orc5* mutant (Fig. 3B) may involve checkpoint systems.

Progression of Distinct Cell Cycle in orc5 Mutants—We performed block and release experiments to examine the effect of the degradation of Orc5p (ORC) on cell cycle progression. Asynchronously cultured *orc5* mutant and wild-type cells were synchronized at G1, S or G2/M phase by incubation with α-factor, HU or nocodazole, respectively. In the *orc5* mutants, Orc5p was supposed to be degraded by incubating cells in YP medium with galactose at 24°C, then at 37°C in the presence of each blocking agent, then cells were released into fresh YP medium with galactose (Fig. 4A). As shown in Fig. 4B, both S phase progression (from HU block) and G2/M phase progression (from nocodazole block) were the same in the *orc5* mutants and wild-type cells. G1/S transition (from α-factor block) was slightly slower in the *orc5* mutants (Fig. 4B). Furthermore, in nocodazole and HU block, although the entry into G1 phase was indistinguishable, the following G1/S transition was delayed in the mutant, suggesting that Orc5p (ORC) is necessary for this step. In *orc5* mutants, the unclear inhibition of G1/S transition (from α-factor block) is probably due to inhibition of the ORC degradation at late G1 phase (at the point of α-factor block); ORC degradation is less in cells blocked with α-factor than in cells blocked with nocodazole, or asynchronously growing cells (data not shown).

To test whether Orc5p (ORC) is necessary for G1/S transition, *orc5* mutant cells, and wild-type cells synchronized at G2/M phase, were incubated at 37°C in YP medium with galactose to degrade Orc5p (ORC), then released into fresh medium with α-factor, to be re-synchronized at late G1 phase, and finally released again into fresh medium to start S phase (Fig. 5A). As shown in Fig. 5B, the G1/S transition was clearly inhibited in *orc5* mutants. In wild type, cells with 2C DNA content peaked within 30 min, and cells with 1C DNA content re-appeared within 100 min of the final release (Fig. 5B). On the other hand, in *orc5* mutants, the peak of DNA content moved gradually from 1C to 2C and cells with 1C DNA content did not reappear (Fig. 5B). These results suggest that when Orc5p (ORC) is depleted from G2/M to late G1, cells can enter G1 normally, but subsequent entry into S phase is inhibited. Thus, ORC must be required for G1/S transition.

Formation of the Pre-RC in the orc5 Mutant—In vivo foot-printing analysis revealed that a protein complex, called pre-RC, is formed in late M or G1 on each origin of chromosomal DNA replication (*35–39*). Pre-RC includes at least ORC, Cdc6p, Cdt1p and MCM (*40*). We here examined the formation of pre-RC in *orc5* degron mutants. We used a chromatin-binding assay to examine the loading of Mcm2p onto chromatin. (Mcm2p is a subunit of MCM). Wild-type cells and *orc5* mutants were synchronized at G2/M, followed by ORC degradation, and finally cells were released into fresh medium (Fig. 6A). As shown in Fig. 6B, in the wild-type cells, Mcm2p bound to chromatin 40 min after the release, and the intensity of band decreased gradually (may be due to cell cycle progression into S and G2/M), consistent with our previous results (*41*). On the other hand, in *orc5* mutants, Mcm2p did not bind chromatin at least until 90 min after the release (Fig. 6B). Thus, when ORC is depleted from G2/M to late G1, pre-RC does not form efficiently. This inefficiency is perhaps what inhibits G1/S transition in the *orc5* mutants (Fig. 5B).

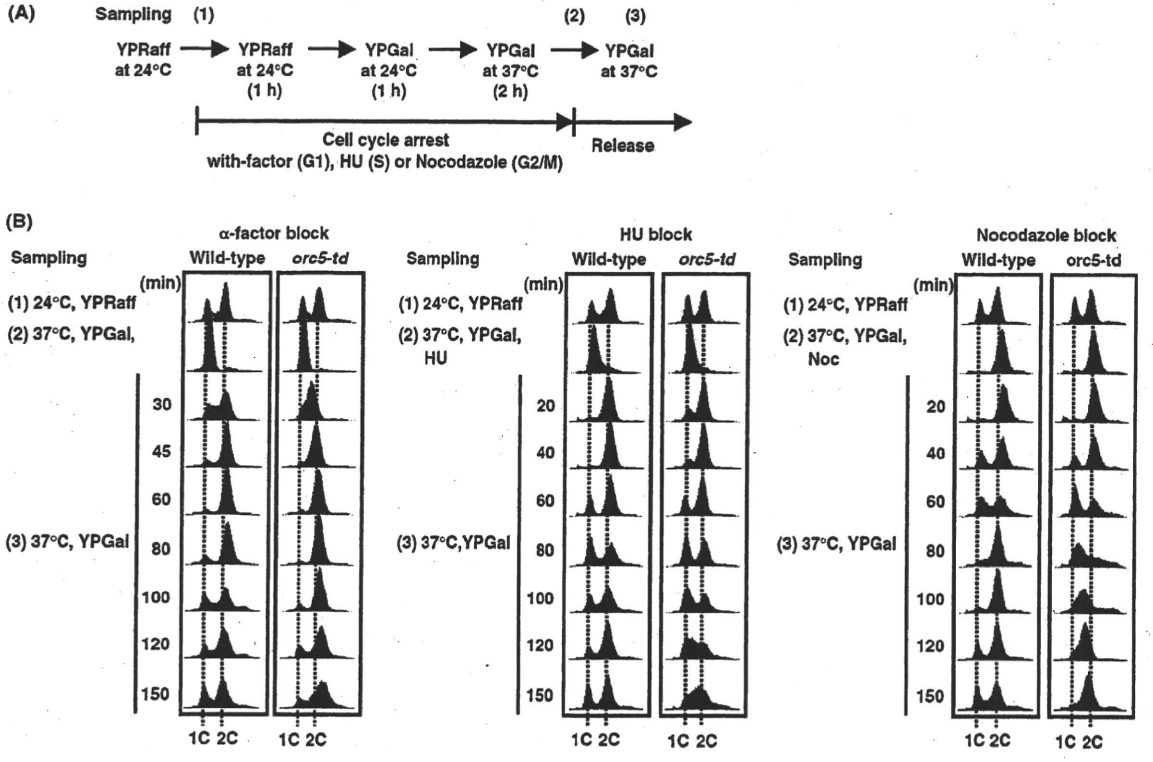

Fig. 4. **Block and release analysis for cell cycle progression in the *orc5* degron mutant.** W303-1A (wild-type) and YYM106 (*orc5-td*) cells were cultured in YP medium with 2% raffinose (YPRaff) to logarithmic phase at 24°C and synchronized at G1, S or G2/M phase by incubation with α-factor, HU or nocodazole, respectively. Cells were cultured first in YPRaff for 1 h at 24°C then in YP medium with 2% galactose (YPGal) for 1 h at 24°C, and finally in the same medium for 2 h at 37°C in the presence of each arrest agent. Cells were washed and released into the fresh YPGal and cultured at 37°C. (A) Experimental outline and timing of sampling. (B) FACS analysis was performed as described in Fig. 3.

ORC is Required at Late G1 Rather Than at Early G1 and G2/M, for Cell Cycle Progression and Pre-RC Formation—In experiments shown in Figs 5 and 6, ORC was absent in both G2/M and the following G1 phases. To define precisely when ORC is required for cell cycle progression (G1/S transition) and pre-RC formation, we designed experiments shown in Fig. 7A; wild-type cells and *orc5* mutants synchronized at G2/M phase, were first incubated in medium with galactose at 37°C to degrade Orc5p (ORC); then released into fresh medium with α-factor to be re-synchronized at G1 phase; then incubated at 24°C in medium with glucose plus α-factor (to restore ORC), or at 37°C in medium with galactose plus α-factor (to keep ORC absent); and finally released into fresh medium to examine cell cycle progression. We used glucose instead of raffinose after the final release, because under these conditions, even wild-type cells grow slowly with raffinose (data not shown). As shown in Fig. 7D, Orc5p was restored by the incubation at 24°C in YP medium with glucose (note the band of Orc5p-td at 60–120 min in the lower right panel in Fig. 7D). Under these conditions, cell cycle progression (G1/S transition) after the final release was identical in *orc5* mutants and wild type (right panel, Fig. 7B) and cells with nearly 2C DNA was not accumulated, even in *orc5* mutants (right panel, Fig. 7B). On the other hand, with continued absence of Orc5p (left panel, Fig. 7B), inhibition of G1/S transition and accumulation of cells with nearly 2C DNA content were observed in the *orc5* mutants, as in Fig. 5B.

We also monitored pre-RC formation under these conditions (Fig. 7C). Following incubation in YP medium with galactose and α-factor at 37°C, both Orc5p and Mcm2p were loaded on chromatin in the wild-type strain, but not in the *orc5* mutant (Fig. 7D, sampling time 3). When *orc5* mutants were subsequently incubated in YP medium with glucose at 24°C to restore Orc5p, both Orc5p and Mcm2p were loaded on chromatin, (lower right panel, Fig. 7D). On the other hand, if the incubation conditions were not shifted (to keep Orc5p absent), neither Orc5p-td nor Mcm2p was loaded on chromatin (lower left panel, Fig. 7D). Thus, for cell cycle progression (G1/S transition) and pre-RC formation, Orc5p (ORC) is required at late G1 (the point of α-factor block), but not at early G1 and G2/M.

Finally, we examined whether pre-RC is degraded after ORC degradation in α-factor-blocked cells. After formation of pre-RC in α-factor-blocked cells, ORC was tried to be degraded by incubation of the *orc5* mutants at 37°C in YP medium with galactose and the level of MCM (Mcm2p) was monitored (Fig. 8A and B). As shown in

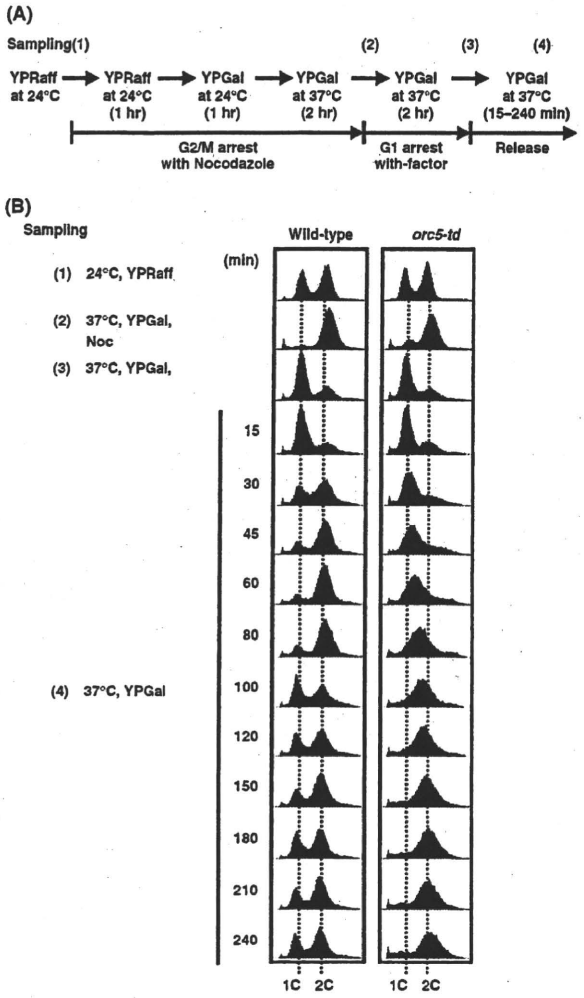

Fig. 5. **Requirement of ORC for G/S transition.** W303-1A (wild-type) and YYM106 (*orc5-td*) cells were cultured in YP medium with 2% raffinose (YPRaff) to logarithmic phase at 24°C and synchronized at G2/M phase by incubation with nocodazole. Cells were cultured first in YPRaff for 1 h at 24°C then in YP medium with 2% galactose (YPGal) for 1 h at 24°C and finally in the same medium for 2 h at 37°C in the presence of nocodazole. Then cells were washed and released into the fresh YPGal containing α-factor and cultured for 2 h at 37°C. Finally, cells were released into the fresh YPGal. (A) Experimental outline and timing of sampling. (B) FACS analysis was performed as described in the legend of Fig. 3.

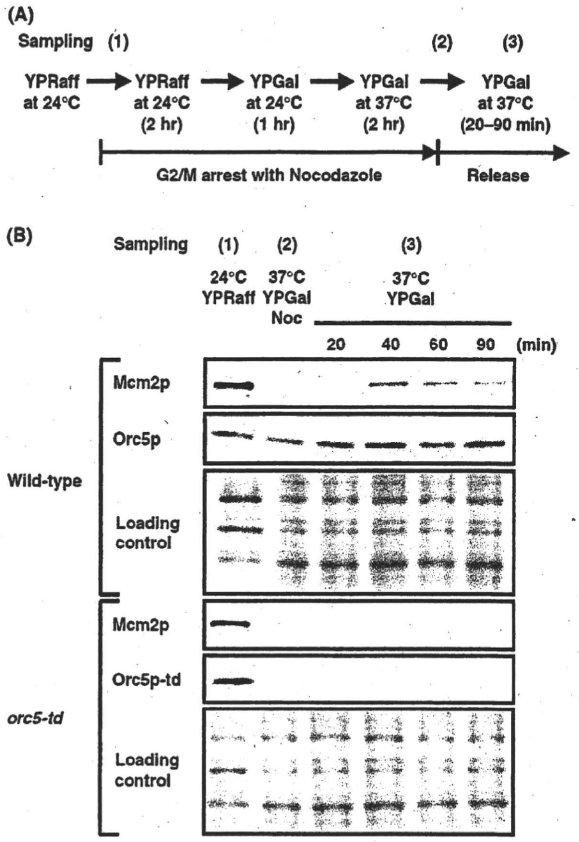

Fig. 6. **The pre-RC formation in the *orc5* degron mutant.** W303-1A (wild-type) and YYM106 (*orc5-td*) cells were cultured in YP medium with 2% raffinose (YPRaff) to logarithmic phase at 24°C and synchronized at G2/M phase by incubation with nocodazole. Cells were cultured first in YPRaff for 2 h at 24°C then in YP medium with 2% galactose (YPGal) for 1 h at 24°C and finally in the same medium for 2 h at 37°C. Cells were washed and released into the fresh YPGal and cultured at 37°C for indicated periods. (A) Experimental outline and timing of sampling. (B) The chromatin loading of Mcm2p and Orc5p monitored by immunoblotting, as described in the legend of Fig. 1. For loading control (bottom panel), gels were stained with silver.

Fig. 8C, Mcm2p released from chromatin more rapidly in *orc5* mutants than in wild-type cells, however, the difference was not so clear. This may be due to that the degradation of Orc5p in *orc5* mutants was not so clear in α-factor-blocked cells as in the nocodazole-blocked cells, as shown in Fig. 8D and E.

DISCUSSION

In yeast, the heat-inducible degron mutant system is very useful to reveal the exact roles of proteins essential for cell growth. This system has helped us to study the functions of various DNA replication-related proteins *in vivo* (*21*, *23*, *24*, *42*), but its application to ORC has not yet been reported. Biochemical studies of ORC have revealed its functions *in vitro*, but, as described in the INTRODUCTION section, genetic studies using temperature-sensitive mutants have so far failed to reveal ORC's precise role *in vivo*. In this study, we constructed a heat-inducible degron mutant for every ORC subunit. All mutants showed temperature-sensitive growth phenotype, confirming that ORC is essential for budding-yeast cell growth. Using these mutants, we examined the role and function of ORC *in vivo*.

In *orc* degron mutants, under the non-permissive conditions, both the targeted ORC subunit, and other subunits, were degraded. Due to technical problems, we

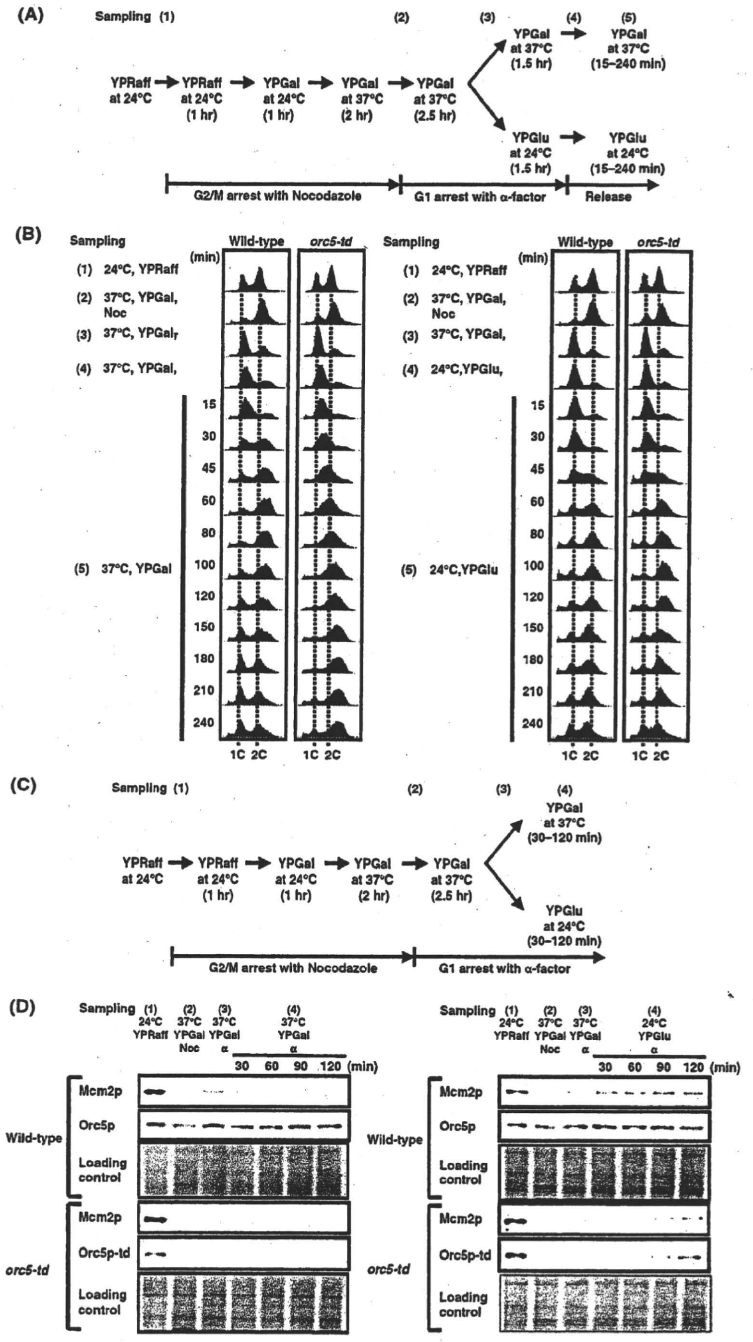

Fig. 7. **The presence of ORC at late G1 rather than early G1 and G2/M phases is important for cell cycle progression and the pre-RC formation.** YYM114 (wild-type) and YYM115 (*orc5-td*) cells were cultured in YP medium with 2% raffinose (YPRaff) to logarithmic phase at 24°C and synchronized at G2/M phase by incubation with nocodazole. Cells were cultured first in YPRaff for 1 h at 24°C then in YP medium with 2% galactose (YPGal) for 1 h at 24°C and finally in the same medium for 2 h at 37°C. Cells were washed and released into the fresh YPGal containing α-factor and cultured for 2.5 h at 37°C. At this point, cell cultures were divided and incubated at 37°C in YPGal with α-factor, or at 24°C in YP medium with 2% glucose (YPGlu) plus α-factor, for 1.5 h (B) or indicated periods (D). Finally, cells were released into fresh YPGal or YPGlu and cultured for indicated periods (B). FACS analysis and chromatin-binding assay was performed as described in the legends of Figs 1 and 3 (B and D). For loading control, gels were stained with silver (D). (A) Experimental outline and timing of sampling for Fig. 7B. (C) Outline and sampling for Fig. 7D.

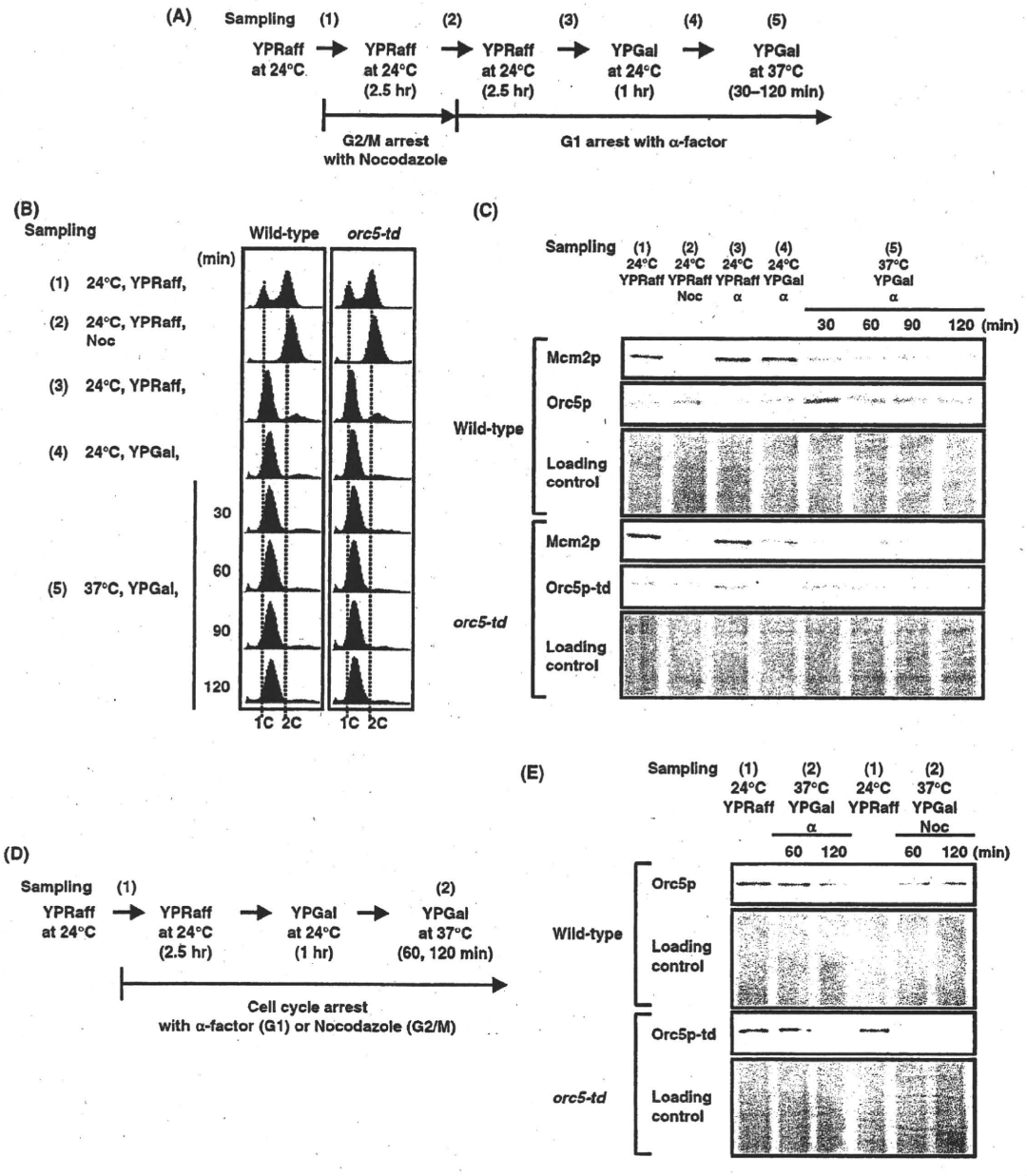

Fig. 8. **Stability of pre-RC after degradation of ORC.** YYM114 (wild-type) and YYM115 (*orc5-td*) cells were cultured in YP medium with 2% raffinose (YPRaff) to logarithmic phase at 24°C and synchronized at G2/M phase by incubation with nocodazole. Cells were washed and released into the fresh YPRaff containing α-factor and cultured for 2.5 h at 24°C, then YP medium with 2% galactose (YPGal) for 1 h at 24°C and finally in the same medium at 37°C for indicated periods. (A) Experimental outline and timing of sampling. (B) FACS analysis. (C) The chromatin loading of Mcm2p and Orc5p monitored by immunoblotting, as described in the legend of Fig. 1. For loading control (bottom panel), gels were stained with silver. YYM114 (wild-type) and YYM115 (*orc5-td*) cells were cultured in YPRaff to logarithmic phase at 24°C and synchronized at G1 phase or G2/M phase by incubation with α-factor or nocodazole for 2.5 h at 24°C, then YPGal for 1 h at 24°C and finally in the same medium at 37°C for indicated periods. (D) Experimental outline and timing of sampling. (E) The Orc5p on chromatin was monitored by immunoblotting, as described in the legend of Fig. 1. For loading control (bottom panel), gels were stained with silver.

could not verify the degradation of all ORC subunits. However, it is reasonable to speculate that under the non-permissive conditions, all subunits of ORC would have been degraded in each of the *orc* degron mutants. Thus, results suggest that ORC probably becomes unstable when any one of its subunits is degraded. We previously reported that in the temperature-sensitive *orc5-A* mutant (a strain expressing ORC with

Orc5pK43E, a mutation in the ATP binding domain of Orc5p), not only Orc5p but also all other subunits were rapidly degraded at non-permissive temperatures by ubiquitin-proteasome system (*15*, *43*). Similar degradation was observed with other temperature-sensitive *orc* mutants (*16*, *44*). Therefore, in yeast, when any one of the ORC subunits is degraded, other subunits may be also degraded by ubiquitin-proteasome system and we speculate that subunits of ORC other than targeted one, are degraded by this system in *orc* degron mutants. But since the same system degrades the targeted subunit, we could not study the degradation of targeted and non-targeted subunits separately.

Block and release experiments suggested that ORC is required for G1/S transition but not for S and G2/M phase progression. Degradation of Orc5p (ORC) at S or G2/M phases did not inhibit the S or G2/M phase progressions, but elimination of Orc5p (ORC) from G2/M to late G1 phase, inhibited the subsequent G1/S transition. This conclusion is consistent with results in many previous studies using temperature-sensitive *orc* mutants, and genetic shut-off systems for Orc6p (*13*, *16–19*, *34*, *45*). As well as various temperature-sensitive *orc* mutants, incubation of asynchronously growing *orc* degron mutant cells under non-permissive conditions, caused accumulation of cells with nearly 2C DNA content. There are two possible explanations. First, as reported for other DNA replication-related mutants (*41*, *46*), inefficient loading of MCM onto chromatin caused by the low level of ORC in *orc* degron mutant cells is responsible for slow S phase progression and accumulation of cells with nearly 2C DNA. Second, the low level of ORC induces DNA damage and the DNA replication checkpoint systems that block cell cycle progression before mitosis. Supporting this idea, we showed that incubation of *orc5* degron mutant cells under non-permissive conditions caused phosphorylation of Rad53p. Furthermore, in other temperature-sensitive *orc* mutants, non-permissive temperatures induce not only DNA damage and DNA replication checkpoint systems, but also spindle assembly checkpoint systems (*14*, *34*). Both possibilities imply that ORC functions primarily as the initiator of DNA replication. The accumulation of cells with nearly 2C DNA content, seen in various temperature-sensitive *orc* mutants, may be due to inefficient MCM loading and/or induction of checkpoint systems.

For cell cycle progression, Orc5p (ORC) is required at late G1 phase rather than early G1 and G2/M phases. Even after elimination of Orc5p (ORC) from G2/M to late G1 (the point of α-factor block), α-factor-blocked *orc5* mutants could enter into S phase normally, after the release, as long as Orc5p (ORC) had been restored before the release. The heat-inducible degron system did not work well in cells blocked with α-factor (i.e. blocked after pre-RC formation). Therefore, we could not test the effect of eliminating Orc5p (ORC) in late G1 on the following G1/S transition. Thus, we do not know whether ORC is required at late G1 for the subsequent G1/S transition. However, recent studies using genetic shut-off systems for Orc6p, showed that the elimination of Orc6p in cells blocked with α-factor did inhibit the subsequent G1/S transition (*45*), suggesting that ORC is required at late G1. Furthermore, we showed that pre-RC can form in cells in late G1 phase provided that Orc5p (ORC) is restored. This is interesting because previous studies suggested that pre-RC is formed in late M or early G1 phase (*29*, *35*). It seems that the pre-RC can be formed in relatively wide window in the cell cycle, from late G2/M (after the decrease in Cdc28p kinase activity) to late G1 (the point of α-factor block). This wide window may help yeast cells to maintain cell cycle progression under stress, which might otherwise inhibit pre-RC formation.

We thank Drs Bruce Stillman (Cold Spring Harbor Laboratory) and John F.X. Diffley (ICRF) for providing plasmids, and antibodies against ORC. This work was supported by Grants-in-Aid for Scientific Research from the Ministry of Education, Culture, Sports, Science and Technology, Japan.

REFERENCES

1. Skarstad, K. and Boye, E. (1994) The initiator protein DnaA: evolution, properties and function. *Biochim. Biophys. Acta* **1217**, 111–130
2. Bell, S.P. and Stillman, B. (1992) ATP-dependent recognition of eukaryotic origins of DNA replication by a multiprotein complex. *Nature* **357**, 128–134
3. Dutta, A. and Bell, S.P. (1997) Initiation of DNA replication in eukaryotic cells. *Annu. Rev. Cell Dev. Biol.* **13**, 293–332
4. Klemm, R.D., Austin, R.J., and Bell, S.P. (1997) Coordinate binding of ATP and origin DNA regulates the ATPase activity of the origin recognition complex. *Cell* **88**, 493–502
5. Sekimizu, K., Bramhill, D., and Kornberg, A. (1987) ATP activates dnaA protein in initiating replication of plasmids bearing the origin of the E. coli chromosome. *Cell* **50**, 259–265
6. Takenaka, H., Makise, M., Kuwae, W., Takahashi, N., Tsuchiya, T., and Mizushima, T. (2004) ADP-binding to origin recognition complex of Saccharomyces cerevisiae. *J. Mol. Biol.* **340**, 29–37
7. Makise, M., Takenaka, H., Kuwae, W., Takahashi, N., Tsuchiya, T., and Mizushima, T. (2003) Kinetics of ATP-binding to Origin Recognition Complex of *Saccharomyces cerevisiae*. *J. Biol. Chem.* **278**, 46440–46445
8. Speck, C., Chen, Z., Li, H., and Stillman, B. (2005) ATPase-dependent cooperative binding of ORC and Cdc6 to origin DNA. *Nat. Struct. Mol. Biol.* **12**, 965–971
9. Klemm, R.D. and Bell, S.P. (2001) ATP bound to the origin recognition complex is important for preRC formation. *Proc. Natl. Acad. Sci. USA* **98**, 8361–8367
10. Bowers, J.L., Randell, J.C., Chen, S., and Bell, S.P. (2004) ATP hydrolysis by ORC catalyzes reiterative Mcm2–7 assembly at a defined origin of replication. *Mol. Cell* **16**, 967–978
11. Randell, J.C., Bowers, J.L., Rodriguez, H.K., and Bell, S.P. (2006) Sequential ATP hydrolysis by Cdc6 and ORC directs loading of the Mcm2–7 helicase. *Mol. Cell* **21**, 29–39
12. Loo, S., Fox, C.A., Rine, J., Kobayashi, R., Stillman, B., and Bell, S. (1995) The origin recognition complex in silencing, cell cycle progression, and DNA replication. *Mol. Biol. Cell* **6**, 741–756
13. Dillin, A. and Rine, J. (1998) Roles for ORC in M phase and S phase. *Science* **279**, 1733–1737
14. Watanabe, K., Morishita, J., Umezu, K., Shirahige, K., and Maki, H. (2002) Involvement of RAD9-dependent damage checkpoint control in arrest of cell cycle, induction of cell death, and chromosome instability caused by defects in origin recognition complex in Saccharomyces cerevisiae. *Eukaryot. Cell* **1**, 200–212

15. Takahashi, N., Yamaguchi, Y., Yamairi, F., Makise, M., Takenaka, H., Tsuchiya, T., and Mizushima, T. (2004) Analysis on origin recognition complex containing Orc5p with defective Walker A motif. *J. Biol. Chem.* **279**, 8469–8477
16. Bell, S.P., Kobayashi, R., and Stillman, B. (1993) Yeast origin recognition complex functions in transcription silencing and DNA replication. *Science* **262**, 1844–1849
17. Liang, C., Weinreich, M., and Stillman, B. (1995) ORC and Cdc6p interact and determine the frequency of initiation of DNA replication in the genome. *Cell* **81**, 667–676
18. Zhang, Y., Yu, Z., Fu, X., and Liang, C. (2002) Noc3p, a bHLH protein, plays an integral role in the initiation of DNA replication in budding yeast. *Cell* **109**, 849–860
19. Foss, M., McNally, F.J., Laurenson, P., and Rine, J. (1993) Origin recognition complex (ORC) in transcriptional silencing and DNA replication in S. cerevisiae. *Science* **262**, 1838–1844
20. Dohmen, R.J., Wu, P., and Varshavsky, A. (1994) Heat-inducible degron: a method for constructing temperature-sensitive mutants. *Science* **263**, 1273–1276
21. Labib, K., Tercero, J.A., and Diffley, J.F. (2000) Uninterrupted MCM2-7 function required for DNA replication fork progression. *Science* **288**, 1643–1647
22. Tercero, J.A., Labib, K., and Diffley, J.F. (2000) DNA synthesis at individual replication forks requires the essential initiation factor Cdc45p. *EMBO J.* **19**, 2082–2093
23. Tanaka, S. and Diffley, J.F. (2002) Interdependent nuclear accumulation of budding yeast Cdt1 and Mcm2–7 during G1 phase. *Nat. Cell Biol.* **4**, 198–207
24. Kanemaki, M., Sanchez-Diaz, A., Gambus, A., and Labib, K. (2003) Functional proteomic identification of DNA replication proteins by induced proteolysis in vivo. *Nature* **423**, 720–724
25. Thomas, B.J. and Rothstein, R. (1989) Elevated recombination rates in transcriptionally active DNA. *Cell* **56**, 619–630
26. Longtine, M.S., McKenzie, A., 3rd., Demarini, D.J., Shah, N.G., Wach, A., Brachat, A., Philippsen, P., and Pringle, J.R. (1998) Additional modules for versatile and economical PCR-based gene deletion and modification in Saccharomyces cerevisiae. *Yeast* **14**, 953–961
27. Sikorski, R.S. and Hieter, P. (1989) A system of shuttle vectors and yeast host strains designed for efficient manipulation of DNA in Saccharomyces cerevisiae. *Genetics* **122**, 19–27
28. Mizushima, T., Takahashi, N., and Stillman, B. (2000) Cdc6p modulates the structure and DNA binding activity of the origin recognition complex in vitro. *Genes Dev.* **14**, 1631–1641
29. Liang, C. and Stillman, B. (1997) Persistent initiation of DNA replication and chromatin-bound MCM proteins during the cell cycle in cdc6 mutants. *Genes Dev.* **11**, 3375–3386
30. Donovan, S., Harwood, J., Drury, L.S., and Diffley, J.F. (1997) Cdc6p-dependent loading of Mcm proteins onto pre-replicative chromatin in budding yeast. *Proc. Natl. Acad. Sci. USA* **94**, 5611–5616
31. Weinreich, M., Liang, C., and Stillman, B. (1999) The Cdc6p nucleotide-binding motif is required for loading mcm proteins onto chromatin. *Proc. Natl. Acad. Sci. USA* **96**, 441–446
32. Hartwell, L.H. and Weinert, T.A. (1989) Checkpoints: controls that ensure the order of cell cycle events. *Science* **246**, 629–634
33. Longhese, M.P., Clerici, M., and Lucchini, G. (2003) The S-phase checkpoint and its regulation in Saccharomyces cerevisiae. *Mutat. Res.* **532**, 41–58
34. Gibson, D.G., Bell, S.P., and Aparicio, O.M. (2006) Cell cycle execution point analysis of ORC function and characterization of the checkpoint response to ORC inactivation in Saccharomyces cerevisiae. *Genes Cells* **11**, 557–573
35. Diffley, J.F., Cocker, J.H., Dowell, S.J., and Rowley, A. (1994) Two steps in the assembly of complexes at yeast replication origins in vivo. *Cell* **78**, 303–316
36. Dahmann, C., Diffley, J.F., and Nasmyth, K.A. (1995) S-phase-promoting cyclin-dependent kinases prevent re-replication by inhibiting the transition of replication origins to a pre-replicative state. *Curr. Biol.* **5**, 1257–1269
37. Stillman, B. (1996) Cell cycle control of DNA replication. *Science* **274**, 1659–1664
38. Diffley, J.F. (1996) Once and only once upon a time: specifying and regulating origins of DNA replication in eukaryotic cells. *Genes Dev.* **10**, 2819–2830
39. Zou, L. and Stillman, B. (1998) Formation of a preinitiation complex by S-phase cyclin DK-dependent loading of Cdc45p onto chromatin. *Science* **280**, 593–596
40. Bell, S.P. and Dutta, A. (2002) DNA replication in eukaryotic cells. *Annu. Rev. Biochem.* **71**, 333–374
41. Takahashi, N., Tsutsumi, S., Tsuchiya, T., Stillman, B., and Mizushima, T. (2002) Functions of sensor 1 and sensor 2 regions of Saccharomyces cerevisiae Cdc6p in vivo and in vitro. *J. Biol. Chem.* **277**, 16033–16040
42. Labib, K., Kearsey, S.E., and Diffley, J.F. (2001) MCM2-7 proteins are essential components of prereplicative complexes that accumulate cooperatively in the nucleus during G1-phase and are required to establish, but not maintain, the S-phase checkpoint. *Mol. Biol. Cell* **12**, 3658–3667
43. Makise, M., Takahashi, N., Matsuda, K., Yamairi, F., Suzuki, K., Tsuchiya, T., and Mizushima, T. (2007) Mechanism for the degradation of origin recognition complex containing Orc5p with a defective Walker A motif and its suppression by over-production of Orc4p in yeast cells. *Biochem. J.* **402**, 397–403
44. Shimada, K., Pasero, P., and Gasser, S.M. (2002) ORC and the intra-S-phase checkpoint: a threshold regulates Rad53p activation in S phase. *Genes Dev.* **16**, 3236–3252
45. Semple, J.W., Da-Silva, L.F., Jervis, E.J., Ah-Kee, J., Al-Attar, H., Kummer, L., Heikkila, J.J., Pasero, P., and Duncker, B.P. (2006) An essential role for Orc6 in DNA replication through maintenance of pre-replicative complexes. *EMBO J.* **25**, 5150–5158
46. Schepers, A. and Diffley, J.F. (2001) Mutational analysis of conserved sequence motifs in the budding yeast Cdc6 protein. *J. Mol. Biol.* **308**, 597–608

Mini Review

Development of new type of NSAIDs with lower gastric side effects

Tohru Mizushima

Graduate School of Medical and Pharmaceutical Sciences, Kumamoto University, Kumamoto, Japan

Non-steroidal anti-inflammatory drugs (NSAIDs) are a useful family of therapeutics. The anti-inflammatory actions of NSAIDs are mediated through their inhibitory effects on cyclooxygenase (COX) activity and resulting decrease in prostaglandins (PGs). On the other hand, NSAID use is associated with gastrointestinal complications. Although PGs have a strong protective effect on gastrointestinal mucosa, the inhibition of COX by NSAIDs is not the sole explanation for the gastrointestinal side effects of NSAIDs. In this study, we examined the COX-independent mechanism involved in NSAID-induced gastric lesions. Using DNA microarray analysis, we found that CHOP, a transcription factor with apoptosis-inducing ability is induced by NSAIDs and treatment of cells with NSAIDs caused apoptosis in wild-type cells but not in CHOP-knock out cells. We also found that NSAIDs have membrane permeabilization activity. Furthermore, intracellular Ca^{2+} chelator, BAPTA-AM inhibited the NSAID-induced apoptosis and induction of CHOP. *In vivo*, we proposed that both COX inhibition at gastric mucosa and direct gastric mucosal cell damage (such as induction of apoptosis) by NSAIDs are required for the production of gastric lesions. Results showed that NSAID-induced apoptosis is mediated by permeabilization of cytoplasmic membranes, increase in the intracellular Ca^{2+} levels and induction of CHOP. Furthermore, results suggest that NSAIDs without membrane permeabilizing activity have reduced gastrointestinal side effects.

Rec.10/17/2007, Acc.11/19/2007, pp100-104

Key words NSAIDs, gastric ulcer, apoptosis, membrane permeabilization

INTRODUCTION

NSAIDs are one of the most frequently used classes of medicines in the world and account for nearly 5% of all prescribed medications[1]. However, NSAID administration is associated with gastrointestinal complications, such as gastric ulcers and bleeding, which sometimes become life-threatening diseases[2]. About 15-30% of chronic users of NSAIDs have gastrointestinal ulcers and bleeding. In the United States, about 16,500 people per year die as a result of NSAID-associated gastrointestinal complications[3]. Therefore, the molecular mechanism governing NSAID-induced gastrointestinal damage needs to be elucidated in order to develop new NSAIDs that do not have these side effects.

Inhibition of COX by NSAIDs, which is responsible for their anti-inflammatory activity was previously thought to be fully responsible for their gastrointestinal side effects[4]. There are at least two subtypes of COX, COX-1 and COX-2, which are responsible for the majority of COX activity at the gastric mucosa and tissues with inflammation, respectively. Therefore, it is reasonable to speculate that selective COX-2 inhibitors have anti-inflammatory activity without gastrointestinal side effects. In fact,

a greatly reduced incidence of gastroduodenal lesions was reported for selective COX-2 inhibitors (such as celecoxib and rofecoxib) both in animal and clinical data[5]. However, the increased incidence of gastrointestinal lesions and the decrease in PG levels induced by NSAIDs are not always linked with each other. For example, higher doses of NSAIDs were required for producing gastric lesions than were required for inhibiting COX at the gastric mucosa[6]. Understanding the additional mechanisms is necessary in order to establish an alternative method for development of gastrointestinally safe NSAIDs other than simply increasing their COX-2 selectivity. This new class of NSAIDs may be clinically beneficial because clinical disadvantages (ie. risk of cardiovascular thrombotic disease) of selective COX-2 inhibitors were recently suggested[7,8] (see below).

In this study, we found that NSAIDs have the direct cytotoxic effect which is independent of the inhibition of COX and dependent on membrane permeabilization activity of NSAIDs and suggest that in addition to COX-inhibition by NSAIDs, direct cytotoxic effect of NSAIDs is involved in NSAID-induced gastric lesions *in vivo*.

RESULTS

1)Direct cytotoxic effect of NSAIDs

Using the primary culture of guinea pig gastric mucosal cells, we examined effect of indomethacin on cell death[9,10]. As shown in Fig.1A, treatment of cells with indomethacin for 1 h decreased cell viability in a dose-dependent manner, but did not affect the size of chromosomal DNA (Fig.1B), even at high concentrations (2.5 mM), suggesting that short-term treatments of gastric mucosal cells with indomethacin induce necrosis. To confirm this finding, we carried out double-staining experiments with PI and Ho 342. Since necrotic cells lose their membrane integrity, PI staining causes pink nuclear staining in necrotic cells. Control cells did not stain with PI but cells treated with 2.5 mM indomethacin for 1 h showed pink nuclear staining (Fig.1C). We also measured the caspase-3 activities by the use of specific fluorogenic peptide substrates. As shown in Fig.1D, cells treated with 2.5 mM indomethacin for 1 h did not showed higher activity of caspase-3. All these results show that short-term treatments of gastric mucosal cells with indomethacin induce necrosis.

On the other hand, treatment of cells with indomethacin for 16 h decreased cell viability in a dose-dependent manner and induced apoptotic DNA fragmentation, apoptotic chromatin condensation and caspase-3 activation (Fig.1A-D), showing that long-term treatments of gastric mucosal cells with indomethacin induce apoptosis.

In order to test whether the cytotoxic effect of NSAIDs (necrosis and apoptosis) are dependent of their ability to inhibit COX, we examined the effect of exogenously added PGE_2 on necrosis and apoptosis induced by indomethacin. Exogenously added PGE_2 did not affect the extent of cell death by short-term or long-term treatment with indomethacin (necrosis or apoptosis, respectively) even at higher concentrations of PGE_2 than is present endogenously in medium[11]. Results suggest that the cytotoxic effect of NSAIDs (necrosis and apoptosis) are independent of their ability to inhibit COX.

2)Membrane permeabilization activity of NSAIDs

We examined membrane permeabilization activity of more than 10 NSAIDs (Nimesulide, celecoxib, mefenamic acid, flufenamic acid, flurbiprofen, indomethacin, diclofenac, etodolac, ibuprofen and ketoprofen) using calcein-loaded liposomes[12,13]. Calcein fluoresces very weakly at high concentrations due to self-quenching, so the addition of membrane permeabilizing drugs to a medium containing calcein-loaded liposomes should cause an increase in fluorescence by diluting out the calcein[12]. All of NSAIDs tested increased the calcein fluorescence, suggesting that they have membrane permeabilization activity. We also examined the necrosis- and apoptosis-inducing ability of these NSAIDs as done for indomethacin in Fig.1. To examine the relationship between NSAID-induced necrosis or apoptosis and membrane permeabilization, we determined ED_{50} values of the 10 NSAIDs for necrosis or apoptosis (concentrations of NSAIDs required for 50% inhibition of cell viability by necrosis or apoptosis) and ED_{20} values for membrane permeabilization (concentration of NSAIDs required for 20% release of calcein). We used ED_{20} values instead of ED_{50} values for estimating the activity of each NSAID for membrane permeabilization because ED_{50} values of etodolac for calcein release could not to be determined. Plotting ED_{50} values for necrosis or apoptosis vs ED_{20} values for membrane permeabilization (calcein release) yielded an r^2 value of 0.94 or 0.93, respectively (Fig.2), which suggests that NSAID-induced necrosis and apoptosis is mediated by their ability to permeabilize membranes.

3)DNA microarray analysis

It is believed that necrosis is induced by drastic permeabilization of cytoplasmic membranes, however, mechanism how membrane permeabilization activity of NSAIDs induces apoptosis remained unclear. In order to understand molecular mechanism governing this apoptosis, we searched for genes whose expression is induced by indomethacin using DNA microarray analy-

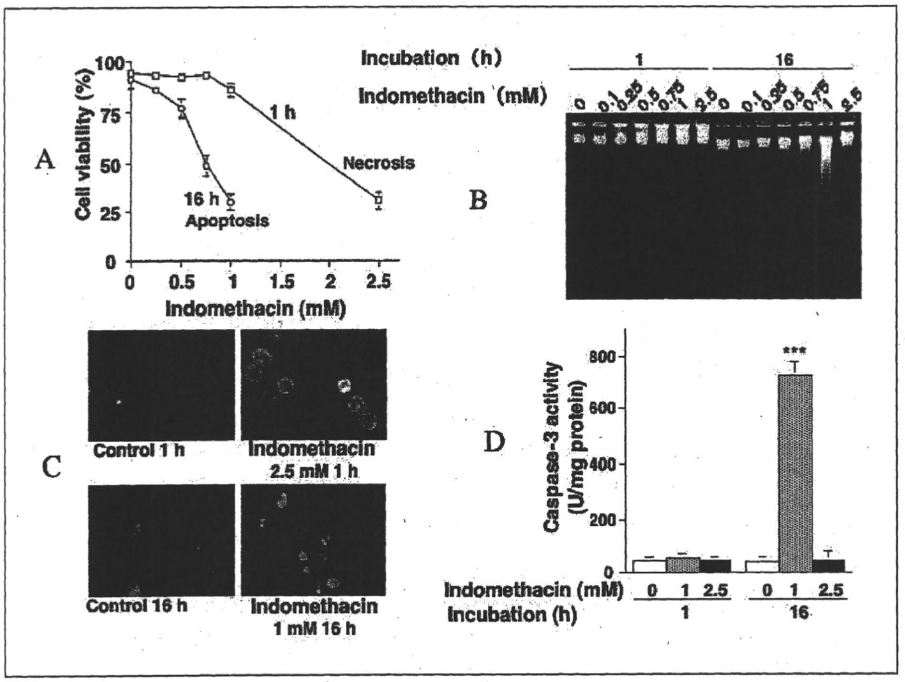

Fig.1 Induction of necrosis and apoptosis by NSAIDs *in vitro*

Cultured gastric mucosal cells were incubated with indicated concentrations of indomethacin for 1 hr or 16 hr. Cell viability was determined by the trypan blue exclusion test (A). Chromosomal DNA was extracted and analyzed by 2% agarose gel electrophoresis (B). After staining with both Ho 342 and PI, cells were observed under fluorescence microscope (C). Cell lysates were prepared and their activity of caspase-3 was measured by fluorometric assay using Ac-DEVD-MCA. Values are mean ± S.E.M. (n=3) (D).

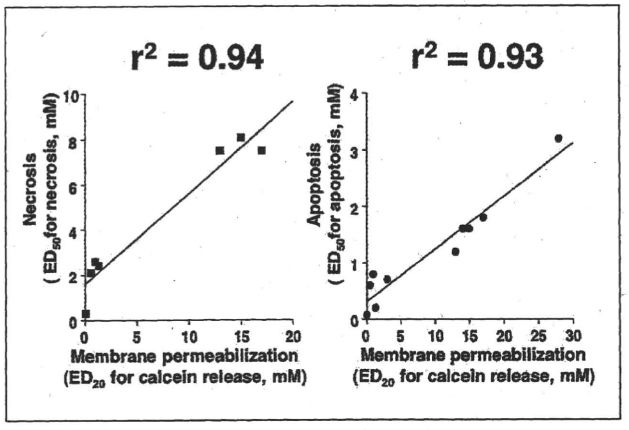

Fig.2 Relationship between necrosis- or apoptosis-inducing and membrane permeabilization activities of NSAIDs

ED_{20} values for membrane permeabilization (calcein release), ED_{50} values for apoptosis and necrosis are calculated and plotted.

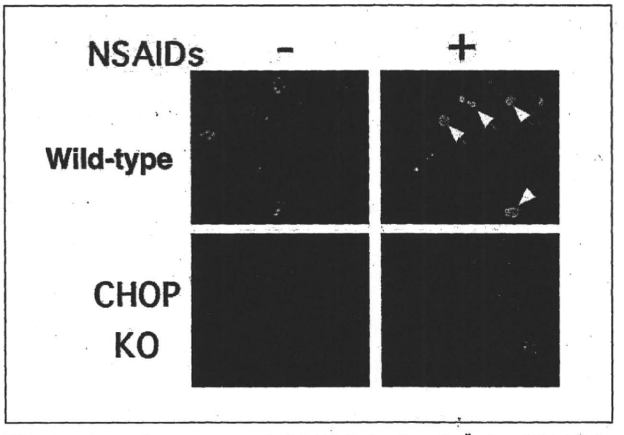

Fig.3 Involvement of CHOP-induction in NSAID-induced apoptosis

Peritoneal macrophages from wild-type or CHOP deficient mice were treated with 1 mM indomethacin for 24 h. Cells were stained with Hoechst dye 33258 and observed under a fluorescence microscope. Arrows indicate condensed chromatins.

sis and found that CHOP, a transcription factor with apoptosis-inducing ability is induced by various NSAIDs[14-16]. The analyses conditions were shown in other paper[14]. In order to test whether the induction of CHOP by indomethacin is involved in indomethacin-induced apoptosis, we used CHOP deficient mice. Peritoneal macrophages from wild-type mice or CHOP deficient mice were treated with indomethacin for 24 h. As shown in Fig.3, indomethacin-induced chromatin condensation was observed in peritoneal macrophages from wild-type mice but not so apparently in those from CHOP deficient mice. This result strongly suggests that the induction of CHOP is involved in NSAID-induced apoptosis.

4)Contribution of the increase in the intracellular Ca^{2+} level

Permeabilization of cytoplasmic membranes causes an increase in intracellular Ca^{2+} levels by stimulating Ca^{2+} influx across the

cytoplasmic membrane and we showed that all of NSAIDs tested increases the intracellular Ca^{2+} level[13]. We used BAPTA-AM, an intracellular Ca^{2+} chelator that is permeable for cytoplasmic membranes to test the contribution of the increase in the intracellular Ca^{2+} level to NSAID-induced apoptosis. BAPTA-AM inhibited NSAID-induced cell death, apoptotic chromatin condensation and induction of CHOP in the presence of NSAIDs[13], suggesting that the increase in intracellular Ca^{2+} levels caused by NSAIDs is involved in NSAID-induced CHOP induction and resulting apoptosis.

5) Development of gastric lesions by a combination of the oral administration of selective COX-2 inhibitors with the intravenous administration of non-selective NSAIDs

We considered that not only COX inhibition (inhibition of PG synthesis) but also the COX-independent direct cytotoxic effect of NSAIDs is involved in the development of gastrointestinal lesions *in vivo*. For testing this idea by pharmacological experiments, it is necessary to separate these two properties of NSAIDs (ie. COX inhibition and direct cytotoxicity) in the model of NSAID-induced gastric lesions *in vivo*. We tried to achieve this by employing intravenous administration of a non-selective NSAID (indomethacin) and oral administration of cytotoxic selective COX-2 inhibitors (such as celecoxib) in rats. Intravenous administration of non-selective NSAIDs may cause inhibition of both COX-1 and COX-2 (thus inhibition of PG synthesis) at the gastric mucosa without any direct cytotoxicity to the gastric mucosa, because the concentration of NSAIDs at the gastric mucosa following intravenous administration is much lower compared to when NSAIDs are orally administered. On the other hand, oral administration of celecoxib may cause direct cytotoxicity to the gastric mucosa without inhibition of COX-1 and thus PG synthesis may be maintained. We also used another selective COX-2 inhibitor, rofecoxib, which shows no cytotoxic effect on gastric mucosal cells[11].

Intravenous administration of indomethacin (3 mg/kg) in rats did not produce gastric lesions (Fig.4) even though the level of PGE_2 at the gastric mucosa was reduced by more than 90%. This data suggests that inhibition of COX is not sufficient to produce gastric lesions. On the other hand, oral administration of celecoxib did not by themselves (ie. without intravenous administration of indomethacin) produce gastric lesions (Fig.4). PGE_2 synthesis at the gastric mucosa was not inhibited by the oral administration of celecoxib. Therefore, the absence of gastric lesions only by oral administration of these selective COX-2 inhibitors can be explained by the fact that inhibition of PG synthesis is required for the development of gastric lesions by NSAIDs.

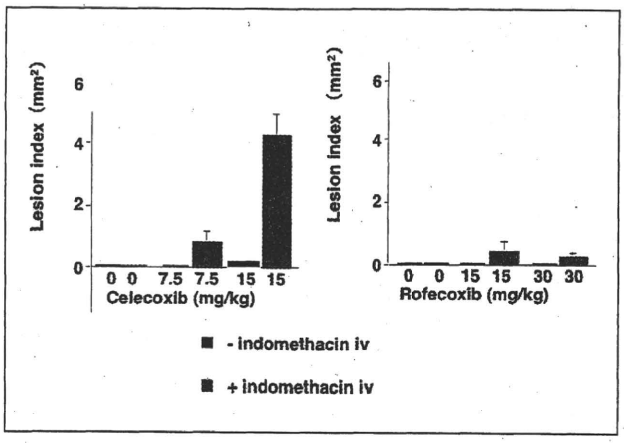

Fig.4 Production of gastric ulcers *in vivo*
Rats were intravenously administered with or without 3 mg/kg indomethacin. After 1 h, animals were orally administered with NSAIDs as indicated. After 6 h, the stomach was removed and scored for hemorrhagic damage. Values are mean ± S.E.M. (n=6).

Interestingly, a combination of intravenous administration of indomethacin and oral administration of celecoxib clearly produced gastric lesions (Fig.4). On the other hand, a combination of intravenous administration of indomethacin and oral administration of rofecoxib did not significantly produce gastric lesions (Fig.4). Results in Fig.4 suggest that direct cytotoxicity of celecoxib but not rofecoxib is involved in production of gastric lesions. All these results support our idea that not only COX inhibition (inhibition of PG synthesis) but also the COX-independent direct cytotoxic effect of NSAIDs is involved in the development of gastric lesions *in vivo*.

CONCLUSION

Results showed that NSAID-induced apoptosis is mediated by permeabilization of cytoplasmic membranes, increase in the intracellular Ca^{2+} levels and induction of CHOP. Furthermore, results suggest that NSAIDs without membrane permeabilizing activity have reduced gastrointestinal side effects. We consider that the concentrations of NSAIDs required for necrosis and apoptosis *in vitro* are possible *in vivo* associating with gastric ulceration in animal models, as discussed in our previous paper[9].

An issue that was recently raised concerning the use of COX-2-selective NSAIDs is their potential risk for promoting cardiovascular thrombotic events[8]. Prostacyclin, a potent anti-aggregator of platelets and a vasodilator, is mainly produced by COX-2 in vascular endothelial cells, while thromboxane A_2, a potent

aggregator of platelets and a vasoconstrictor, is mainly produced by COX-1 in platelets[17]. Until recently, rofecoxib and celecoxib were leading COX-2 selective NSAIDs in the market. Rofecoxib was withdrawn from the market due to the risk of it promoting cardiovascular thrombotic events and the U. S. Food and Drug Administration (FDA) advised physicians to consider alternatives to celecoxib due to the risk of it causing cardiovascular thrombotic events[18]. Based on our findings, NSAIDs that do not exhibit membrane permeabilization activity may be safe for the gastrointestinal tract even if they are not highly selective for COX-2. This type of NSAID may be of clinical benefit because they are predicted to be safe for both the gastrointestinal tract and cardiovascular system. We are now chemically synthesizing such NSAIDs.

References

1) Smalley WE, Ray WA, Daugherty JR, Griffin MR: Nonsteroidal anti-inflammatory drugs and the incidence of hospitalizations for peptic ulcer disease in elderly persons. Am J Epidemiol, 141: 539-545, 1995.
2) Hawkey CJ: Nonsteroidal anti-inflammatory drug gastropathy. Gastroenterology, 119: 521-535, 2000.
3) Singh G: Recent considerations in nonsteroidal anti-inflammatory drug gastropathy. Am J Med, 105: 31S-38S, 1998.
4) Hoshino T, Tsutsumi S, Tomisato W, Hwang HJ, Tsuchiya T, Mizushima T: Prostaglandin E2 protects gastric mucosal cells from apoptosis via EP2 and EP4 receptor activation. J Biol Chem, 278: 12752-12758, 2003.
5) Chan CC, Boyce S, Brideau C, Charleson S, Cromlish W, Ethier D, Evans J, Ford-Hutchinson AW, Forrest MJ, Gauthier JY, Gordon R, Gresser M, Guay J, Kargman S, Kennedy B, Leblanc Y, Leger S, Mancini J, O'Neill GP, Ouellet M, Patrick D, Percival MD, Perrier H, Prasit P, Rodger I, et al: Rofecoxib [Vioxx, MK-0966; 4-(4'-methylsulfonylphenyl)-3-phenyl-2-(5H)-furanone]: a potent and orally active cyclooxygenase-2 inhibitor. Pharmacological and biochemical profiles. J Pharmacol Exp Ther, 290: 551-560, 1999.
6) Ligumsky M, Golanska EM, Hansen DG, Kauffman GJ: Aspirin can inhibit gastric mucosal cyclo-oxygenase without causing lesions in rat. Gastroenterology, 84: 756-761, 1983.
7) Mukherjee D, Nissen SE, Topol EJ: Risk of cardiovascular events associated with selective COX-2 inhibitors. JAMA, 286: 954-959, 2001.
8) Mukherjee D: Selective cyclooxygenase-2 (COX-2) inhibitors and potential risk of cardiovascular events. Biochem Pharmacol, 63: 817-821, 2002.
9) Tomisato W, Tsutsumi S, Rokutan K, Tsuchiya T, Mizushima T: NSAIDs induce both necrosis and apoptosis in guinea pig gastric mucosal cells in primary culture. Am J Physiol Gastrointest Liver Physiol, 281: G1092-G1100, 2001.
10) Aburaya M, Tanaka K, Hoshino T, Tsutsumi S, Suzuki K, Makise M, Akagi R, Mizushima T: Heme oxygenase-1 protects gastric mucosal cells against non-steroidal anti-inflammatory drugs. J Biol Chem, 281: 33422-33432, 2006.
11) Tomisato W, Tsutsumi S, Hoshino T, Hwang HJ, Mio M, Tsuchiya T, Mizushima T: Role of direct cytotoxic effects of NSAIDs in the induction of gastric lesions. Biochem Pharmacol, 67: 575-585, 2004.
12) Tomisato W, Tanaka K, Katsu T, Kakuta H, Sasaki K, Tsutsumi S, Hoshino T, Aburaya M, Li D, Tsuchiya T, Suzuki K, Yokomizo K, Mizushima T: Membrane permeabilization by non-steroidal anti-inflammatory drugs. Biochem Biophys Res Commun, 323: 1032-1039, 2004.
13) Tanaka K, Tomisato W, Hoshino T, Ishihara T, Namba T, Aburaya M, Katsu T, Suzuki K, Tsutsumi S, Mizushima T: Involvement of intracellular Ca^{2+} levels in nonsteroidal anti-inflammatory drug-induced apoptosis. J Biol Chem, 280: 31059-31067, 2005.
14) Mima S, Tsutsumi S, Ushijima H, Takeda M, Fukuda I, Yokomizo K, Suzuki K, Sano K, Nakanishi T, Tomisato W, Tsuchiya T, Mizushima T: Induction of claudin-4 by nonsteroidal anti-inflammatory drugs and its contribution to their chemopreventive effect. Cancer Res, 65: 1868-1876, 2005.
15) Tsutsumi S, Gotoh T, Tomisato W, Mima S, Hoshino T, Hwang HJ, Takenaka H, Tsuchiya T, Mori M, Mizushima T: Endoplasmic reticulum stress response is involved in nonsteroidal anti-inflammatory drug-induced apoptosis. Cell Death Differ, 11: 1009-1016, 2004.
16) Namb, T, Hoshino T, Tanaka K, Tsutsumi S, Ishihara T, Mima S, Suzuki K, Ogawa S, Mizushima T: Up-regulation of 150-kDa oxygen-regulated protein by celecoxib in human gastric carcinoma cells. Mol Pharmacol, 71: 860-870, 2007.
17) Belton O, Byrne D, Kearney D, Leahy A, Fitzgerald DJ: Cyclooxygenase-1 and -2-dependent prostacyclin formation in patients with atherosclerosis. Circulation, 102: 840-845, 2000.
18) Ray WA, Griffin MR, Stein CM: Cardiovascular toxicity of valdecoxib. N Engl J Med, 351: 2767, 2004.

JOURNAL OF BACTERIOLOGY, Jan. 2008, p. 648–654 Vol. 190, No. 2
0021-9193/08/$08.00+0 doi:10.1128/JB.01513-07
Copyright © 2008, American Society for Microbiology. All Rights Reserved.

SmdAB, a Heterodimeric ABC-Type Multidrug Efflux Pump, in *Serratia marcescens*▽

Taira Matsuo,[1,2] Jing Chen,[2] Yusuke Minato,[2] Wakano Ogawa,[2] Tohru Mizushima,[2]† Teruo Kuroda,[1]* and Tomofusa Tsuchiya[2]

Department of Genome Applied Microbiology[1] and Department of Molecular Microbiology,[2] Graduate School of Medicine, Dentistry and Pharmaceutical Sciences, Okayama University, Tsushima, Okayama, 700-8530, Japan

Received 19 September 2007/Accepted 5 November 2007

We cloned genes, designated *smdAB*, that encode a multidrug efflux pump from the chromosomal DNA of clinically isolated *Serratia marcescens* NUSM8906. For cells of the drug-hypersensitive strain *Escherichia coli* KAM32 harboring a recombinant plasmid carrying *smdAB*, structurally unrelated antimicrobial agents such as norfloxacin, tetracycline, 4′,6-diamidino-2-phenylindole (DAPI), and Hoechst 33342 showed elevated MICs. The deduced amino acid sequences of both SmdA and SmdB exhibited similarities to the sequences of ATP-binding cassette (ABC)-type multidrug efflux pumps. The efflux of DAPI and Hoechst 33342 from *E. coli* cells expressing SmdAB was observed, and the efflux activities were inhibited by sodium *o*-vanadate, which is a well-known ATPase inhibitor. The introduction of *smdA* or *smdB* alone into *E. coli* KAM32 did not elevate the MIC of DAPI; thus, both SmdA and SmdB were required for function. These results indicate that SmdAB is probably a heterodimeric multidrug efflux pump of the ABC family in *S. marcescens*.

Drug resistance in bacteria is a serious problem in the hospital setting. In particular, multidrug resistance causes difficulty in the treatment of infectious diseases. There are several mechanisms by which bacterial cells escape the toxicities of antimicrobial agents. Such mechanisms include the degradation or modification of the drugs, the alteration of targets, the emergence of alternative pathways, and the efflux of drugs out of the cells. Among the drug resistance mechanisms, drug efflux is a major cause of multidrug resistance and has been found to play a major role in the intrinsic resistance of many bacteria (28, 31).

Serratia marcescens is a cause of nosocomial and opportunistic infections. It has previously been reported to be associated with respiratory tract infections, urinary tract infections, septicemia, meningitis, and wound infections (9). This organism shows high-level intrinsic resistance to a variety of antimicrobial agents, which makes the treatment of infections with this bacterium very difficult. Previously, we compared the MICs of various antimicrobial agents for several strains of *S. marcescens* with those for *Escherichia coli* and *Pseudomonas aeruginosa* (6). Many antimicrobial agents, such as ampicillin, chloramphenicol, erythromycin, tetracycline, and ethidium bromide, showed higher MICs for *S. marcescens* than for *E. coli*. The levels of drug resistance in *S. marcescens* are roughly comparable to those in *P. aeruginosa*, which shows high-level intrinsic resistance to many antimicrobial agents. Since multidrug efflux pumps have been shown to contribute to the intrinsic resistance of *P. aeruginosa* (19, 20, 28), it may be possible that these pumps are also important for the intrinsic drug resistance of *S. marcescens*.

We have previously reported that we succeeded in the cloning of nine distinct types of genes from the chromosome of *S. marcescens* and that such genes are responsible for drug resistance (6). These genes include *sdeXY* (5), which is a member of the resistance-nodulation-cell division family, and *smfY* (37), which is a member of the major-facilitator superfamily. In addition, Kumar and Worobec have reported the characterization of SdeAB (15). Given the genome sequence of *S. marcescens* Db11, which has been reported by the *S. marcescens* Db11-Sequencing Group at the Sanger Institute (ftp://ftp.sanger.ac.uk/pub/pathogens/sm/), many other multidrug efflux pumps that have not been physiologically characterized are expected to be present.

Another family of multidrug efflux pumps is the ATP-binding cassette (ABC) family. The ABC-type multidrug efflux pumps in eukaryotes have been well characterized and have previously been shown to be involved in tolerance to various cytotoxic agents (22). The human P-glycoprotein is a representative of the eukaryotic ABC-type multidrug efflux pumps (4, 41). The ABC-type multidrug efflux pumps utilize ATP as the energy source and are thus primary transporters. Meanwhile, most of the prokaryotic multidrug transporters are secondary transporters. Some ABC-type drug efflux pumps in prokaryotes, especially in gram-positive bacteria, have been characterized in detail previously (23, 25, 35, 38, 39, 42). These include LmrCD of *Lactococcus lactis*, which has been shown to be involved in intrinsic resistance to some antimicrobial agents (21). In addition, three ABC-type drug efflux pumps in gram-negative bacteria have been reported previously: MacAB, MsbA, and VcaM. MacAB is a macrolide-specific efflux pump and has been identified in several gram-negative bacteria, such as *E. coli*, *Salmonella enterica* serovar Typhimurium, and *Neisseria gonorrhoeae* (14, 29, 30, 34). MacA belongs to the membrane fusion protein family, and MacB is an integral mem-

* Corresponding author. Mailing address: Department of Genome Applied Microbiology, Graduate School of Medicine, Dentistry and Pharmaceutical Sciences, Okayama University, Tsushima, Okayama, 700-8530, Japan. Phone and fax: 81-86-251-7958. E-mail: tkuroda@cc.okayama-u.ac.jp.

† Present address: Graduate School of Medical and Pharmaceutical Sciences, Kumamoto University, Kumamoto, 862-0973, Japan.

▽ Published ahead of print on 16 November 2007.

34

brane protein with a nucleotide-binding domain. MacAB seems to form a tripartite complex together with TolC, which is a multifunctional outer membrane protein in *E. coli* (13). MsbA is an essential ABC-type pump in *E. coli* and is involved in the transport of lipopolysaccharides and phospholipids (43). Furthermore, Reuter et al. demonstrated that MsbA confers multidrug resistance upon *E. coli* and mediates the transport of ethidium from cells (33). We have previously cloned and characterized a multidrug efflux pump, VcaM, from non-O1 *Vibrio cholerae* (10). MsbA and VcaM probably function as homodimers, similar to LmrA of *L. lactis*.

Here, we report the properties of an ABC-type multidrug efflux pump, SmdAB of *S. marcescens*. This pump rendered host *E. coli* cells resistant to various antimicrobial agents. Moreover, SmdAB probably functions as a heterodimer. To our knowledge, this is the first report of an ABC-type pump functioning as a heterodimer in gram-negative bacteria.

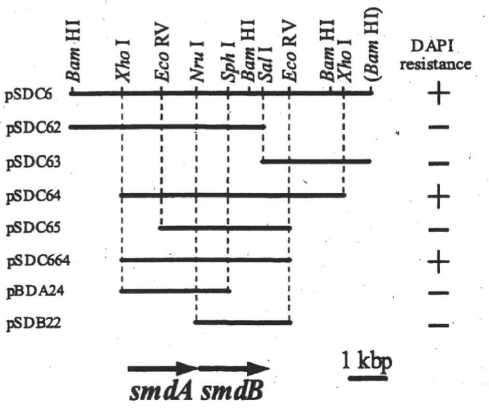

FIG. 1. Restriction map of pSDC6 and its derivatives. DNA regions derived from *S. marcescens* chromosomal DNA and carried by each plasmid are shown. The ability of *E. coli* KAM32 cells harboring each plasmid to grow in L broth containing 0.5 μg of DAPI/ml is indicated on the right; plus signs indicate that cells grew, and minus signs indicate that cells did not grow. The positions and directions of the *smdAB* genes as revealed by sequencing are shown at the bottom.

MATERIALS AND METHODS

Bacterial strains and growth. A clinically isolated *S. marcescens* strain, NUSM8906, was used as the source of chromosomal DNA (6). *E. coli* KAM32 (*ΔacrB ΔydhE hsdΔ5*), which lacks the major multidrug efflux pumps AcrAB and YdhE, is hypersusceptible to many antimicrobial agents (7). *E. coli* KAM42 (*ΔacrB ΔydhE hsdΔ5 ΔtolC*), a *tolC*-deficient strain derived from KAM32, was constructed as described previously (32). Cells were grown in Luria (L) broth (18) at 37°C under aerobic conditions.

An environmentally isolated strain, *S. marcescens* Db10, was a kind gift from Jonathan Ewbank of the Centre d'Immunologie de Marseille Luminy, France.

Cloning, sequencing, and gene manipulation. Genes responsible for resistance to antimicrobial agents were cloned from the chromosome of *S. marcescens* (6). Briefly, chromosomal DNA was prepared from *S. marcescens* NUSM8906 by the method of Berns and Thomas (2). The DNA was partially digested with Sau3AI, and the fragments from 4 to 10 kbp were separated by sucrose density gradient centrifugation. Plasmid pSTV28 (TaKaRa BIO Inc.) was used as a cloning vector. This vector carries *cat*, the chloramphenicol acetyltransferase gene. Plasmid pSTV28 was digested with BamHI, dephosphorylated with bacterial alkaline phosphatase, and then ligated with the chromosomal DNA fragments by using a ligation kit (version 2; TaKaRa BIO Inc.). Competent cells of *E. coli* KAM32 were transformed with the recombinant plasmids and were spread onto 1.5% agar plates containing L broth, 20 μg of chloramphenicol/ml, and 0.5 μg of 4′,6-diamidino-2-phenyindole (DAPI)/ml. The plates were incubated at 37°C for 24 h. We obtained eight candidate hybrid plasmids and selected one of them, named pSDC6.

The DNA insert in plasmid pSDC6 was digested with several restriction endonucleases and subcloned into pSTV28. The resulting plasmids, which had shorter inserts than the original pSDC6 plasmid, were introduced into *E. coli* KAM32 cells, and all transformants were tested for their susceptibilities to DAPI. Of the plasmids that conferred resistance to DAPI upon *E. coli* KAM32, pSDC664 carried the shortest insert and was used for further analysis.

The nucleotide sequence was determined by the dideoxy chain termination method (36) using a DNA sequencer (ALF Express; Pharmacia Biotech). Sequence data were analyzed with GENETYX sequence analysis software (Software Development Co.).

Drug susceptibility tests. The MICs of various antimicrobial agents were determined by using the microdilution method according to the recommendations of the Japanese Society of Chemotherapy (12). Briefly, MICs were determined in Mueller-Hinton broth (Difco) containing each compound in a twofold serial dilution series. The cells were incubated in the test medium at 37°C for 24 h, and growth was examined visually. The MIC of each compound was defined as the lowest concentration that prevented visible growth.

Efflux assays. The DAPI efflux assay was carried out as described previously (16). Briefly, cells of *E. coli* KAM32 harboring control or recombinant plasmids were grown in 20 ml of L broth containing 20 μg of chloramphenicol/ml and 0.5 mM isopropyl β-D-thiogalactopyranoside (IPTG) until the optical density at 650 nm reached 0.7 units. After the cells were harvested, they were washed with modified Tanaka buffer (27, 40) and were then resuspended in the same buffer containing 5 μM DAPI and 1 mM 2,4-dinitrophenol (DNP) and incubated at 37°C for 10 h. DNP, which is a well-known conductor of protons across the cytoplasmic membrane (1), was used to de-energize the cells. The cells were washed with modified Tanaka buffer and then resuspended in the same buffer to obtain an optical density at 650 nm of 0.4 units. The fluorescence of DAPI was measured at excitation and emission wavelengths of 355 and 457 nm, respectively, with a fluorescence spectrophotometer, model F-2000 (Hitachi). The fluorescence intensity of DAPI is higher when DAPI binds to DNA molecules. Thus, the efflux of DAPI from the cell can be monitored by the detection of a decrease in the level of fluorescence over time. The cell suspension was incubated at 37°C for 5 min, and then glucose at 20 mM was added as an energy source to monitor the efflux of DAPI.

The assay for the efflux of Hoechst 33342 was carried out as described previously (10). Briefly, cells were cultured and washed as described above. Washed cells were resuspended in modified Tanaka buffer containing 1 μM Hoechst 33342 and 1 mM DNP and incubated at 37°C for 10 h. The cells were washed with 100 mM 3-morpholinopropanesulfonic acid-tetramethylammonium hydroxide (MOPS-TMAH) containing 1 μM Hoechst 33342 and then resuspended in the same buffer to obtain an optical density at 650 nm of 0.4 units. The fluorescence of Hoechst 33342 was measured at excitation and emission wavelengths of 355 and 457 nm, respectively.

To evaluate the effects of sodium *o*-vanadate on the efflux of DAPI or Hoechst 33342, cell suspensions were prepared in the same way as described above. The cell suspensions were preincubated for 5 min at 37°C with different concentrations of sodium *o*-vanadate (0 to 3 mM) prior to the addition of glucose.

RT-PCR analysis. Total RNA from cells of *S. marcescens* NUSM8906 and Db10 that were grown in L broth until the exponential growth phase was extracted by using the QIAGEN RNeasy mini kit. For efficient RNA extraction, the cells were well broken using a QIAshredder (QIAGEN Inc.) prior to the extraction of RNA. The extracted total RNA was used for reverse transcription-PCR (RT-PCR) with the QIAGEN one-step RT-PCR kit. PCR without the RT reaction was performed to confirm the lack of detectable DNA contamination. RT-PCR products were analyzed by 3% agarose 21 gel (Nippon Gene Co.) electrophoresis.

Nucleotide sequence accession number. The nucleotide sequence data reported in this paper have been deposited in the DDBJ, EMBL, and GenBank nucleotide sequence databases with the accession no. AB360548.

RESULTS

Cloning of *smdAB* and sequence analysis. To understand the role of multidrug efflux pumps in the intrinsic multidrug resistance of *S. marcescens*, it is important to identify multidrug efflux pump genes. We previously cloned nine distinct types of genes from the chromosome of *S. marcescens* NUSU8906 and found that such genes are responsible for drug resistances (6).

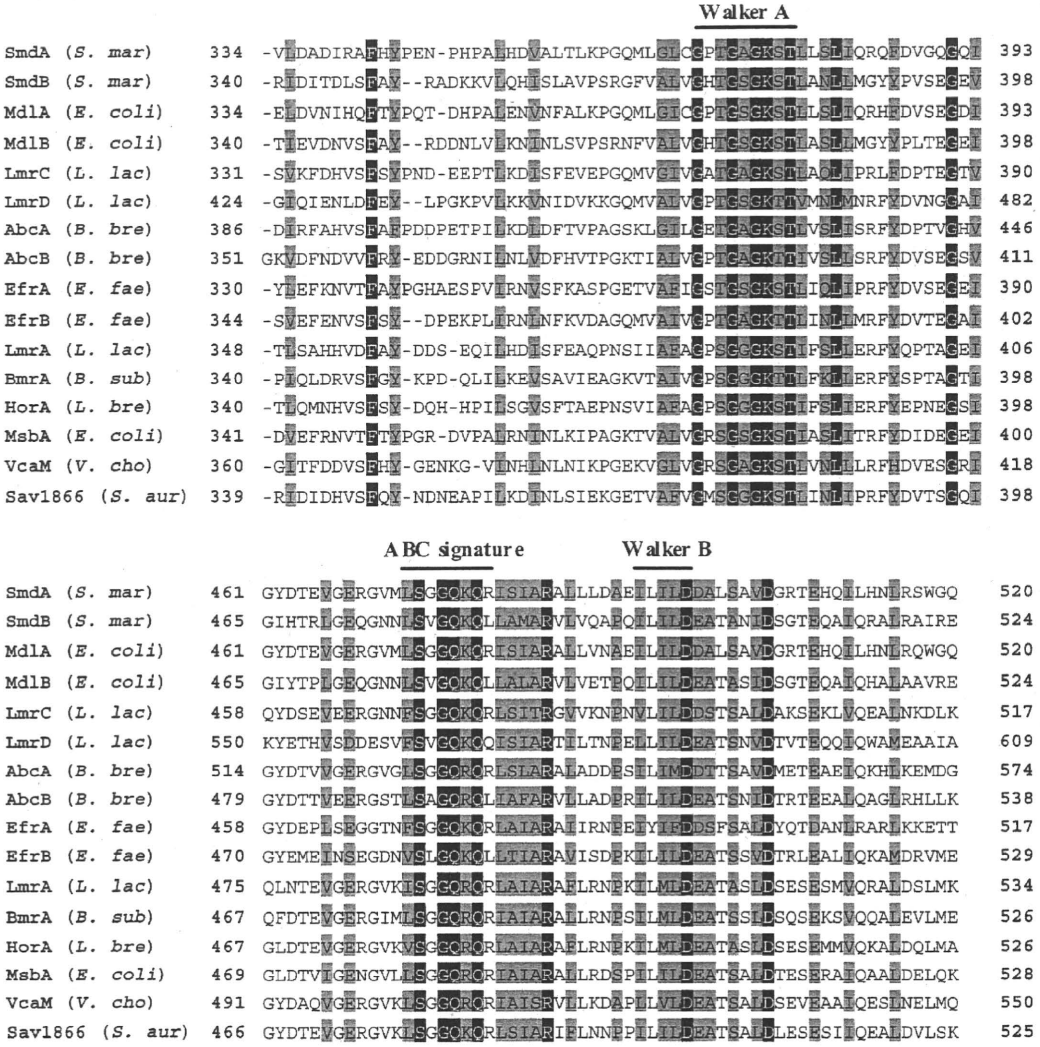

FIG. 2. Multiple-sequence alignments of SmdA, SmdB, and similar or putative proteins. The amino acid sequence alignments of the Walker A motif, the Walker B motif, and the ABC signature sequences are shown. Identical and similar residues are indicated with black and gray backgrounds, respectively. Gaps in the alignment are indicated by hyphens. The numbers on the left and right of the sequences indicate the beginning and ending positions of each sequence, respectively. The sequences were aligned by using the EMBL ClustalW program (available at http://decypher.stanford.edu/decypher/algo-cw/cw_ax.shtml). The names of the organisms from which the proteins are derived are shown in Table 1. *S. mar*, *S. marcescens*; *L. lac*, *L. lactis*; *B. bre*, *Bifidobacterium breve*; *E. fae*, *Enterococcus faecalis*; *B. sub*, *Bacillus subtilis*; *L. bre*, *Lactobacillus brevis*; *V. cho*, *V. cholerae*; *S. aur*, *Staphylococcus aureus*.

One of the recombinant plasmids, pSDC6, rendered *E. coli* KAM32 cells resistant to DAPI, norfloxacin, and tetracycline. Judging from the spectrum of drug resistance, it seemed that the plasmid pSDC6 carried other genes different from *sdeXY* and *smfY*, which we had already reported (5, 37). Thus, we analyzed pSDC6 further.

Plasmid pSDC6 carries a DNA insert about 8 kbp long. We constructed a series of deletion plasmids carrying various portions of the DNA insert in pSDC6 and tested whether those plasmids conferred DAPI resistance upon *E. coli* cells (Fig. 1). Plasmid pSDC664 carried the shortest DNA insert that conferred DAPI resistance. The sequencing of this insert revealed two open reading frames (ORFs). We designated the ORFs *smdA* and *smdB* (for *Serratia multidrug* resistance). The putative gene products were estimated to comprise 591 and 592 amino acid residues, respectively. Only the *smdA* gene has a promoter-like sequence in its upstream region, and both genes have ribosome-binding sequences (Shine-Dalgarno sequences), each of which is followed by a start codon. The *smdB* gene is followed by a transcription terminator-like (inverted repeat) sequence. The two ORFs overlap by 5 nucleotides. Hydropathy analysis by the method of Eisenberg et al. (8) suggested that both SmdA and SmdB possess six putative transmembrane segments followed by hydrophilic segments (data not shown). The hydrophilic segments of both SmdA and SmdB contain putative nucleotide-binding domains, Walker A and Walker B motifs, and ABC signature sequences (11) (Fig. 2).

The comparison of our sequence with the genome sequence of *S. marcescens* Db11 (a streptomycin-resistant mutant of Db10) (ftp://ftp.sanger.ac.uk/pub/pathogens/sm/) showed that

TABLE 1. Sequence similarities to SmdA and SmdB

Transporter	Organism	% Identity to SmdA	% Similarity to SmdA	% Identity to SmdB	% Similarity to SmdB	Reference or accession no.
SmdA	*S. marcescens*			27	70	This study
SmdB	*S. marcescens*	27	70			This study
MdlA	*E. coli*	79	96	26	68	P77265
MdlB	*E. coli*	26	70	79	96	P0AAG5
LmrC	*L. lactis*	26	68	22	67	AAK04408
LmrD	*L. lactis*	26	71	24	64	AAK04409
EfrA	*Enterococcus faecalis*	26	70	24	69	NP_816538
EfrB	*Enterococcus faecalis*	27	66	28	70	NP_816537
AbcA	*Bifidobacterium breve*	17	33	27	67	DQ486860
AbcB	*Bifidobacterium breve*	28	70	29	71	DQ486860
BmrA	*Bacillus subtilis*	28	68	27	69	D70031
HorA	*Lactobacillus brevis*	27	68	24	62	AB005752
LmrA	*L. lactis*	26	70	26	64	U63741
MsbA	*E. coli*	28	69	27	68	P27299
VcaM	*V. cholerae*	27	68	26	68	AB073220
MDR1 (N)[a]	*Homo sapiens*	23	56	23	58	P08183
MDR1 (C)[a]	*Homo sapiens*	26	67	25	66	P08183

[a] N, N-terminal half; C, C-terminal half.

smdA corresponded to SMA0354 and *smdB* to SMA0355. Eighty differences in the nucleotide sequences of *smdA* and SMA0354 and 83 differences between those of *smdB* and SMA0355 were identified. Almost all of these differences were translationally silent, but nine and six amino acid residues were different, respectively. In addition, the ORF of *smdB* was 132 nucleotides shorter than that of SMA0355. SmdA and SmdB showed 27% identity and 70% similarity to each other. A BLAST search of the NCBI database for protein sequence similarities showed SmdA to be 79% identical to MdlA and SmdB to be 79% identical to MdlB of *E. coli*. The search also showed both SmdA and SmdB to have nearly 30% identity to other ABC-type multidrug efflux pumps (Table 1). The levels of similarity in the nucleotide-binding domains were much higher than those in the transmembrane domains.

We also investigated the expression of *smdAB* in *S. marcescens* NUSM8906 (a clinical isolate) and Db10 (an environmental isolate). RT-PCR analysis showed that *smdAB* was expressed to similar extents in the two strains (data not shown).

Drug susceptibility. To investigate the contribution of SmdAB to drug resistance, we measured the MICs of various antimicrobial agents for *E. coli* KAM32 cells to which the plasmid carrying *smdAB* had been introduced. The MICs for *E. coli* KAM32 cells harboring pSDC664 (which carries *smdAB*) or pSTV28 (control) are shown in Table 2. For *E. coli* KAM32 cells, the introduction of the plasmid pSDC664 elevated the MICs of several structurally unrelated drugs: norfloxacin, tetracycline, Hoechst 33342, and tetraphenylphosphonium chloride (TPPCl), in addition to DAPI. Therefore, we concluded that SmdAB conferred multidrug resistance upon *E. coli* KAM32.

MacAB is the sole pump in *E. coli* characterized as an ABC-type drug efflux pump (14). MacAB has previously been shown to require the outer membrane component TolC for function. We therefore investigated whether TolC was required for the function of SmdAB. *E. coli* KAM42 is a *tolC*-lacking strain derived from strain KAM32. The introduction of the plasmid pSDC664 into cells of *E. coli* KAM42 resulted in elevated MICs of various antimicrobial agents, similar to those for *E. coli* KAM32 (data not shown). Thus, we conclude that TolC is not necessary for the function of SmdAB.

To test whether both SmdA and SmdB are necessary for the pump function, we constructed plasmids carrying each one of the corresponding genes. Plasmid pBDA24 carried *smdA*, while plasmid pSDB22 carried *smdB*. Both plasmids were introduced into *E. coli* KAM32 cells. The *smdA* gene was located under the control of the *tet* promoter in the pBR322 vector, and *smdB* was located under the control of the *lac* promoter in the pSTV28 vector (Fig. 1). Since vectors pBR322 and pSTV28 were compatible, both plasmids could be retained simultaneously. The drugs tested did not show elevated MICs for either the KAM32 transformant harboring pBDA24 (carrying *smdA*) or the KAM32 transformant harboring pSDB22 (carrying *smdB*) (Table 3). On the other hand, norfloxacin, tetracycline, TPPCl, and Hoechst 33342 showed elevated MICs for the KAM32 transformant harboring both pBDA24 and pSDB22, similar to those for KAM32 harboring pSDC664 (carrying *smdAB*). Thus, we conclude that both SmdA and SmdB are necessary for resistance.

TABLE 2. MICs of various antimicrobial agents for *E. coli* KAM32/pSTV28 and KAM32/pSDC664

Antimicrobial agent	MIC (μg/ml) for:		Increase (*n*-fold) in MIC[a]
	KAM32/pSTV28	KAM32/pSDC664	
DAPI	0.25	8	32
Norfloxacin	0.016	0.125	8
Ciprofloxacin	0.002	0.004	2
Ofloxacin	0.016	0.016	1
Nalidixic acid	1	1	1
Tetracycline	0.25	2	8
Streptomycin	2	2	1
Erythromycin	4	4	1
Ampicillin	2	2	1
Hoechst 33342	0.25	4	16
TPPCl	4	16	4
Acriflavine	2	2	1

[a] Increase in MIC for *E. coli* KAM32/pSDC664 compared to that for *E. coli* KAM32/pSTV28.

TABLE 3. MICs of various antimicrobial agents for *E. coli* KAM32 cells carrying *smdA* and/or *smdB*

Antimicrobial agent	MIC (μg/ml) for:			
	KAM32/pSTV28 (negative control)	KAM32/pBDA24 (carrying *smdA*)	KAM32/pSDB22 (carrying *smdB*)	KAM32/pBDA24/pSDB22 (carrying *smdA* and *smdB*)
DAPI	0.25	0.25	0.25	8
Norfloxacin	0.016	0.016	0.016	0.125
Tetracycline	0.25	0.25	0.25	2
Hoechst 33342	0.25	0.25	0.25	4
TPPCl	4	4	4	16

Efflux of DAPI and Hoechst 33342. In order to show that SmdAB is a multidrug efflux pump, we measured the efflux of DAPI and Hoechst 33342. Cells of *E. coli* KAM32 harboring either pSDC664 (carrying *smdAB*) or pSTV28 (control) were de-energized and preloaded with DAPI. The addition of glucose as an energy source caused the rapid extrusion of DAPI from KAM32 cells harboring pSDC664 compared with that from KAM32 cells harboring pSTV28 (Fig. 3A). When we measured the efflux of Hoechst 33342, we obtained a similar result (Fig. 3B). The addition of lactate instead of glucose as an energy source caused similar levels of extrusion (data not shown). These results indicate that SmdAB is an energy-dependent multidrug efflux pump.

Inhibition of SmdAB-mediated DAPI efflux by vanadate. From the primary amino acid sequence, SmdAB was categorized within the ABC family of multidrug efflux pumps. The activities of some ABC-type multidrug efflux pumps have previously been reported to be inhibited by sodium *o*-vanadate, an inhibitor of some ATPases (10, 17, 26, 35, 39, 42). We investigated the effect of sodium *o*-vanadate on the DAPI efflux activity of SmdAB. As shown in Fig. 4, sodium *o*-vanadate inhibited the activity in a concentration-dependent manner. The concentration causing 50% inhibition was approximately 1.1 mM. This 50% inhibitory concentration of sodium *o*-vanadate is similar to those for other ABC-type multidrug efflux pumps (10, 17). Meanwhile, Hoechst 33342 efflux activity was also inhibited by sodium *o*-vanadate (data not shown). Thus, it seems that SmdAB is an ATP-dependent multidrug efflux pump of *S. marcescens*.

DISCUSSION

We previously cloned genes that conferred multidrug resistance upon drug-hypersusceptible *E. coli* cells (6). We designated the genes *smdAB* and characterized the properties of SmdAB. SmdAB was categorized into the ABC family of multidrug efflux pumps according to the primary structure. Both SmdA and SmdB were found to contain putative nucleotide-binding domains, Walker A and Walker B motifs, and ABC signature sequences (11) (Fig. 2). We observed the elevation of the MICs of several antimicrobial agents for cells into which *smdAB* was introduced and detected energy-dependent efflux of DAPI and Hoechst 33342 in these cells. The efflux of DAPI and Hoechst 33342 mediated by SmdAB was inhibited by sodium *o*-vanadate, which is a known ATPase inhibitor. Thus, we conclude that SmdAB is an ABC-type multidrug efflux pump. We found that both SmdA and SmdB were necessary for pump function. To our knowledge, SmdAB is the first example of a probably heterodimeric ABC-type multidrug efflux pump in gram-negative bacteria.

Several ABC-type multidrug efflux pumps have been cloned from gram-positive bacteria and characterized previously (10, 14, 17, 23, 25, 29, 33, 35, 38, 39, 42). Among them, LmrCD in *L. lactis* has been demonstrated to be a heterodimeric ABC-type multidrug efflux pump and to contain two structurally and functionally distinct nucleotide-binding domains (24). In LmrD, a canonical glutamate residue following the Walker B motif, which has been postulated to fulfill a critical catalytic role in the hydrolysis of ATP (3), is conserved, but in LmrC,

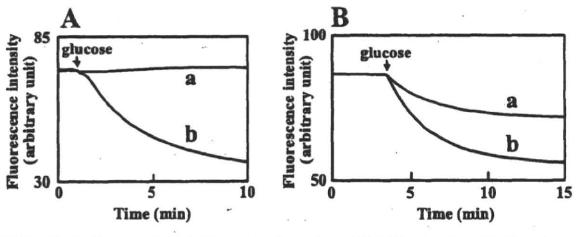

FIG. 3. Efflux of DAPI and Hoechst 33342 via SmdAB. Energy-starved *E. coli* KAM32 cells harboring pSDC664 (carrying *smdAB*) (curves b) or KAM32 cells harboring pSTV28 (control) (curves a) were loaded with 5 μM DAPI (panel A) or 1 μM Hoechst 33342 (panel B). At the time point indicated by the arrow, glucose (final concentration, 20 mM) was added to energize the cells. The fluorescence of dyes at 37°C over time was monitored with a fluorescence spectrophotometer. The downward deflection indicates the efflux of DAPI or Hoechst 33342 from the cells.

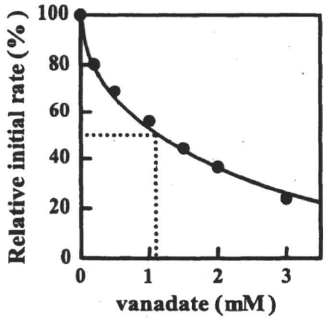

FIG. 4. Inhibition of DAPI efflux activity by sodium *o*-vanadate. Various concentrations of sodium *o*-vanadate were added to the assay mixture, and the mixture was preincubated with the cells for 5 min. Glucose (final concentration, 20 mM) was added to initiate the assay. The relative initial velocity of DAPI efflux was measured. The initial velocity observed in the absence of an inhibitor was set at 100%. Dotted lines indicate IC_{50} (approximately 1.1 mM).